Finite-Length Algebraic Spatially-Coupled Quasi-Cyclic LDPC Codes

Keke Liu, *Member, IEEE,* Mostafa El-Khamy, *Senior Member, IEEE,* and Jungwon Lee, *Senior Member, IEEE*

***Abstract*—The 'replicate-and-mask' (R&M) construction of finite-length spatially-coupled (SC) LDPC codes is proposed in this paper. The proposed R&M construction generalizes the conventional matrix unwrapping construction and contains it as a special case. The R&M construction of a class of algebraic spatially-coupled (SC) quasi-cyclic (QC) LDPC codes over arbitrary finite fields is demonstrated. The girth, rank, and time-varying periodicity of the proposed R&M SC QC LDPC codes are analyzed. The error rate performance of finite-length non-binary algebraic SC QC LDPC codes is investigated with window decoding. Compared to the conventional unwrapping construction, it is found through numerical simulations that the R&M construction resulted in SC QC LDPC codes with better block error rate performance and lower error floors. With a flooding schedule decoder, it is shown that the proposed R&M algebraic SC QC LDPC codes have better error performance than the corresponding LDPC block codes and random SC codes. The R&M construction of irregular SC QC LDPC codes is demonstrated. It is shown that low-complexity regular puncturing schemes can be deployed on these codes to construct families of rate-compatible irregular SC QC LDPC codes with good performance.**

***Index Terms*—LDPC codes, algebraic LDPC codes, quasi-cyclic codes, spatially-coupled LDPC codes, girth, PEG algorithm, rate-compatible codes, HARQ**

I. Introduction

SPATIALLY-coupled low-density parity-check (SC LDPC) codes, originally known as LDPC convolutional codes [2], have received much attention due to their excellent thresholds. It has been proved [3], [4], [5], [6] that for binary memoryless symmetric (BMS) channels, the maximum a posteriori probability (MAP) threshold of a regular LDPC [7] block ensemble can be approached by the belief propagation (BP) threshold of an ensemble generated by spatially coupling a collection of the original LDPC block ensembles. This is called the *threshold saturation phenomenon*. In addition to the asymptotic performance analysis, the finite-length performance of SC LDPC codes, especially decoded using window decoding methods, has also become a focal point of research [8], [9].

Manuscript received ....; revised ...., and ....; accepted .... Date of current version November 6, 2015. The review of this paper was coordinated by ....

K. Liu was with the Department of Electrical and Computer Engineering, University of California, Davis, CA, USA, and held an internship in Modem R&D, Samsung Electronics, San Diego, CA. He is currently with Avago Technologies, San Jose, CA. (e-mail: kkeliu@ucdavis.edu)

M. El-Khamy is with Modem R&D, Samsung Electronics, San Diego, CA 92121, USA. He is also with the Department of Electrical Engineering, Alexandria University, Alexandria 21544, Egypt. (e-mail: mostafa.e@samsung.com)

J. Lee is with Modem R&D, Samsung Electronics, San Diego, CA 92121, USA. He is also with the Electrical and Computer Engineering Department, University of California, San Diego, CA, USA. (e-mail: jungwon2.lee@samsung.com)

This work was presented in part at the IEEE International Symposium on Information Theory (ISIT 2014), July 2014 [1].

Quasi-cyclic (QC) LDPC codes [10] have been standardized for various communication systems and are appearing in recent data storage products, due to their low complexity and highly parallelizable encoding [11] and decoding [12]. Extensive simulation results [13], [14], [15] have shown that well-designed QC LDPC codes can perform as well as (or even better than) unstructured random LDPC codes. Simulation results have also shown that non-binary protograph LDPC block codes can outperform their binary counterparts [16].

Due to the merits of both QC LDPC codes and SC LDPC codes, this paper addresses the construction of SC LDPC codes with a QC structure, over arbitrary finite fields. Such codes are called SC QC LDPC codes. There are not many prior works addressing the construction of SC QC LDPC codes. Mitchell *et al.* presented a technique that improves the upper bound on the minimum Hamming distance of members of the QC sub-ensembles [17]. The progressive edge growth (PEG) algorithm [18], which usually requires a significantly long computer search, has been modified to construct binary SC QC LDPC codes [19]. Recently, M. Hagiwara *et al.* proposed a construction of SC QC LDPC codes for quantum error correction [20], which is, to the best knowledge of the authors, the only existing work that constructs SC QC LDPC codes using a deterministic approach. However, this construction is specific to a small class of special matrices, and is not flexible enough for arbitrary code design.

Besides the above-mentioned works, a natural method of constructing SC QC LDPC codes is to unwrap a QC LDPC block code [21], [2]. We will refer to such codes as unwrapped SC QC LDPC codes. The unwrapping construction can preserve many structural properties of the underlying block code, such as the girth and the minimum distance [21], [22]. However, we discovered that with window decoding (WD), unwrapped SC QC LDPC block codes could start to show error floors at a block error rate (BLER) of 10^{-2}, which is the operating BLER of many wireless communication systems. This is undesirable since the throughput of many communication systems, especially those deploying hybrid automatic repeat request (HARQ) mechanisms, is determined by the BLER rather than the bit error rate (BER). This issue will be addressed in this paper.

In this paper, we present a systematic construction of SC LDPC codes called the *replicate and mask* (R&M) construction, which is our main contribution. We will refer to such SC codes constructed with the R&M construction as R&M SC LDPC codes. The crux of the R&M construction is replicating the parity-check (PC) matrix of an LDPC block code and masking it with a designed masking matrix. Compared to the conventional unwrapping approach, we show that the proposed R&M construction provides more flexibility in the selection of the code parameters, such as the rate and degree distributions, and the optimization of the constructed codes. The R&M SC LDPC codes can also be guaranteed to have certain girth properties. The conventional unwrapping technique is shown to be a special instance of our new construction approach. Then, we combine our new R&M construction approach with the classical algebraic construction of QC LDPC codes [13], [14], [15], [23] to present a general algebraic construction of SC QC LDPC codes over arbitrary finite fields. In contrast to the previous PEG-based constructions [19], our construction of SC QC LDPC codes avoids time-consuming computer search. Compared to the construction in [20], our construction results in a much larger class of SC QC LDPC codes with a more flexible parameter selection. We illustrate the R&M construction of different SC QC LDPC codes by examples. It is shown that the constructed regular R&M SC QC LDPC codes outperform both the corresponding LDPC block codes and random SC codes with the flooding schedule decoding (FSD) [24]. For the case of WD [9], [8], [25], it is shown that regular R&M SC QC LDPC codes outperform the corresponding unwrapped SC QC LDPC codes, especially at the error floor region. We also show that the R&M SC QC LDPC codes are robust to puncturing, and hence we construct families of rate-compatible (RC) SC QC LDPC codes suitable for wireless HARQ systems with low complexity regular puncturing. For that, we also demonstrate how to construct irregular SC QC LDPC codes with the R&M construction. To our knowledge, this is the first time irregular SC QC LDPC codes are constructed.

This paper is one of few works addressing the finite length construction of non-binary spatially coupled LDPC codes and investigating their performance on the binary input additive white Gaussian noise channel (BI-AWGNC). This work shows that SC codes can have a better error-rate performance than their block code counterparts at finite length. This work has been partially motivated by their promising asymptotic length performance. The asymptotic performance of non-binary SC codes has been studied on the binary erasure channel (BEC), where it has been shown that the threshold saturation phenomenon also holds for non-binary SC LDPC codes on the BEC [26]. We numerically showed in [1] that the threshold saturation phenomenon also holds for (particular ensembles of) non-binary SC LDPC codes on the BI-AWGNC using a flooding-schedule decoder. Specifically, it has been numerically shown that for the (3,6)-regular block code ensemble, as the spatial-coupling length increases, the belief propagation threshold of the spatially coupled non-binary code over GF(2^2) approaches an upper bound on the MAP threshold of the corresponding non-binary block code on the BI-AWGNC [1]. Moreover, it has been recently shown that WD of non-binary SC codes, on both the BI-AWGNC and the BEC, results in a negligible degradation in their decoding thresholds compared to the FSD if the window size is sufficiently large [25].

The rest of this paper is organized as follows. The unwrapping construction of SC LDPC codes is briefly reviewed in Section II. The general R&M construction of SC LDPC codes is presented in Section III, and the general algebraic construction of SC QC LDPC codes over arbitrary finite fields is discussed in Section IV. Certain characteristics of the R&M constructions are also proved in Sections III and IV. Various examples for the R&M construction of regular, irregular, and rate-compatible SC QC LDPC codes are shown in Section V, together with their FSD error rate performance. Their WD error rate performance is investigated in Section VI. Concluding remarks are made in Section VII.

II. Background: Spatially-coupled LDPC codes and Unwrapping Construction

Let G be a (d_v, d_c)-regular protograph [27], where d_v and d_c denote the variable node (VN) and check node (CN) degrees, respectively. The protograph G_{sc} of a (d_v, d_c, L) SC LDPC code is obtained by spatially coupling a chain of L copies of G [3].

A well-known approach to construct SC LDPC codes from LDPC block codes is based on matrix unwrapping [21], [2]. [1] Let $\mathbf{H}$ be the PC matrix of an LDPC block code, and suppose $\mathbf{H}$ can be decomposed into a set of $\mathcal{L}$ matrices $\{\mathbf{H}_i\}_{0\leq i<\mathcal{L}}$ such that $\mathbf{H} = \sum_{i=0}^{\mathcal{L}-1} \mathbf{H}_i$ (in $\mathbb{Z}$). We arrange $\{\mathbf{H}_i\}_{0\leq i<\mathcal{L}}$ in such a way that a band-diagonal array is formed, as follows,

$$\mathbf{H}_{sc} = \begin{bmatrix} \mathbf{H}_0 & & & & & \\ \mathbf{H}_1 & \mathbf{H}_0 & & & & \\ \vdots & \vdots & \ddots & & & \\ \mathbf{H}_{\mathcal{L}-1} & \mathbf{H}_{\mathcal{L}-2} & \cdots & \mathbf{H}_0 & & \\ & \mathbf{H}_{\mathcal{L}-1} & \mathbf{H}_{\mathcal{L}-2} & \cdots & \mathbf{H}_0 & \\ & & & \ddots & \ddots & \ddots \end{bmatrix}. \quad (1)$$

It is observed from (1) that, if we neglect the effect of termination, the unwrapped SC LDPC code has the same code rate and degree distributions as the underlying LDPC block code.

III. A 'Replicate-and-Mask' Construction of binary SC LDPC codes

In this section, we present a systematic construction of SC LDPC codes, referred to as the *replicate and mask* (R&M) construction. The proposed R&M construction is based on *masking a replicated version of an LDPC block code using a masking matrix that is closely dependent on the target SC protograph*. (The relation between the masking matrix and the SC protograph will be clarified in Section III-A.) Compared to the matrix unwrapping techniques, our R&M construction has more flexibility in the choice of the underlying block code, and has more degrees of freedom in optimizing the constructed SC LDPC codes. The proposed R&M construction generalizes the conventional matrix unwrapping construction and contains it as a special instance.

Since many notations are introduced in this section, the important notations are summarized in Table I.

[1] In fact, the approach of [21] generalizes the idea of matrix unwrapping originally proposed in [2]. For simplicity of presentation in this paper, by 'unwrapping' we mean the generalized approach of [21].

This article has been accepted for publication in a future issue of this journal, but has not been fully edited. Content may change prior to final publication. Citation information: DOI 10.1109/JSAC.2015.2504273, IEEE Journal on Selected Areas in Communications

TABLE I
SUMMARY OF NOTATIONS USED IN SECTION III

Notation	Explanation
$\mathbf{H}$,M,N	$\mathbf{H} = [h_{i,j}]_{0\leq i<M,0\leq j<N}$ is the $M \times N$ PC matrix of the LDPC block code used in the R&M construction described in Algorithm 1.
$\mathbf{H}_{rep}$	$\mathbf{H}_{rep} = [h_{rep,i,j}]_{0\leq i,j<\infty}$ is a semi-infinite two-dimensional array of $\mathbf{H}$.
$\mathbf{W}$,S,T	$\mathbf{W} = [w_{i,j}]_{0\leq i<S,0\leq j<T}$ is the $S \times T$ masking matrix used in the R&M construction described in Algorithm 1.
$\mathbf{H}_{sc}$	$\mathbf{H}_{sc} = [h_{sc,i,j}]_{0\leq i<S,0\leq j<T}$ is the PC matrix of the constructed SC LDPC code.
Q	Lifting size of the constructed protograph SC LDPC code where the protograph is constructed to have single edges between nodes
$\{\Sigma_k\}$, A, B, C, L	A band-diagonal $\mathbf{W}$ consists of L $A \times B$ binary component matrices $\{\Sigma_k\}$ ($0 \leq k < L$) with the 'step size' C, where $\Sigma_k = [\sigma_{i,j,k}]_{0\leq i<A,0\leq j<B}$ for $0 \leq k < L$.
$\mathcal{T}$	The block periodicity of $\mathbf{H}_{sc}$. See Lemma 3 for more details.

A. A general R&M construction of SC LDPC codes

Consider a finite field GF(q). Let $\mathbf{H} = [h_{i,j}]_{0\leq i<M,0\leq j<N}$ be an $M \times N$ matrix over GF(2). First, *replicate* $\mathbf{H}$ to form the following semi-infinite array $\mathbf{H}_{rep}$:

$$\mathbf{H}_{rep} = [h_{rep,i,j}]_{0\leq i,j<\infty} = \begin{bmatrix} \mathbf{H} & \mathbf{H} & \mathbf{H} & \cdots \\ \mathbf{H} & \mathbf{H} & \mathbf{H} & \cdots \\ \mathbf{H} & \mathbf{H} & \mathbf{H} & \cdots \\ \vdots & \vdots & \vdots & \ddots \end{bmatrix} \quad (2)$$

where $h_{rep,i,j} = h_{(i \bmod M),(j \bmod N)}$ for all $i, j \geq 0$.

Consider a *masking matrix* $\mathbf{W} = [w_{i,j}]_{0\leq i<S,0\leq j<T}$, which is a binary matrix of size $S \times T$ and has a 'band-diagonal' pattern. Let $\mathbf{H}_{rep}(S,T)$ denote the $S \times T$ submatrix of $\mathbf{H}_{rep}$, taken from the upper left corner of $\mathbf{H}_{rep}$. We can construct an $S \times T$ SC PC matrix $\mathbf{H}_{sc}$ by masking $\mathbf{H}_{rep}(S,T)$ using $\mathbf{W}$, i.e., $\mathbf{H}_{sc} = [h_{sc,i,j}]_{0\leq i<S,0\leq j<T} = \mathbf{H}_{rep}(S,T) \circ \mathbf{W}$, where '$\circ$' denotes the Hadamard product [28] (i.e., entry-wise product of two matrices), and $h_{sc,i,j} = h_{rep,i,j} \cdot w_{i,j}$ for $0 \leq i < S$ and $0 \leq j < T$, *cf.* Fig. 1(e). We refer to the above process as the 'replicate-and-mask' (R&M) construction, and summarize it in Algorithm 1. Fig.1 illustrates an example of the R&M construction of SC LDPC codes.

Typically, a masking matrix $\mathbf{W}$ with a band-diagonal pattern consists of L $A\times B$ binary component matrices $\{\Sigma_k\}$ ($0 \leq k < L$) with the 'step size' C, where $\Sigma_k = [\sigma_{i,j,k}]_{0\leq i<A,0\leq j<B}$ for $0 \leq k < L$. In this case, $S = CL + (A - C)$, $T = BL$, and $\mathbf{W} = [w_{i,j}]_{0\leq i<(CL+(A-C)),0\leq j<BL}$, where for $\mathcal{J} \equiv (kC \leq i < kC + A)\&(kB \leq j < (k+1)B)$ for $0 \leq k < L$

$$w_{i,j} = \begin{cases} \sigma_{i-kC,j-kB,k} & \text{if } \mathcal{J}, \\ 0 & \text{otherwise.} \end{cases} \quad (3)$$

The R&M construction can also be used to construct SC codes from a SC protomatrix. In general, consider a SC protomatrix $\mathbf{H}'_{sc}$ whose corresponding SC protograph does not have more than one edge between any VN and CN pair. Such an SC protograph with single edge between nodes can always be found by lifting another SC protograph with multiple edges. Suppose we would like to construct a protograph-based SC LDPC code with SC protomatrix $\mathbf{H}'_{sc}$ and lifting size Q, $Q \geq 1$. Then, we first construct the masking matrix $\mathbf{W}$ by replacing each 1-entry and 0-entry in $\mathbf{H}'_{sc}$ by an all-one $Q\times Q$ matrix and a $Q\times Q$ zero matrix (ZM), respectively. Then, $\mathbf{H}$ is chosen to be an $m \times n$ array of $Q \times Q$ permutation matrices, i.e., $M = mQ$ and $N = nQ$. The block matrix $\mathbf{H}$ is then used together with the masking matrix $\mathbf{W}$ in the R&M construction to result in the PC matrix $\mathbf{H}_{sc}$ of a protograph-based SC LDPC code with lifting size Q.

It is worth mentioning that the proposed R&M method essentially exists for constructing LDPC block codes. For example, the LDPC block code constructions based on column splitting [29] and dispersion [30], can be viewed as special cases of the R&M construction. However, this work is the first to construct R&M SC LDPC codes.

Algorithm 1 R&M construction of SC LDPC codes

1: Construct a PC matrix $\mathbf{H}$ of an LDPC block code over GF(2) that has the desired girth property.
2: Replicate $\mathbf{H}$ to form a two-dimensional semi-infinite array $\mathbf{H}_{rep}$ of $\mathbf{H}$ as in (2).
3: Design an $S \times T$ masking matrix $\mathbf{W}$ with binary elements and the desired band-diagonal pattern.
4: Take an $S \times T$ submatrix $\mathbf{H}_{rep}(S,T)$ of $\mathbf{H}_{rep}$ from the upper left corner of $\mathbf{H}_{rep}$.
5: Mask $\mathbf{H}_{rep}(S,T)$ using $\mathbf{W}$ to obtain an SC PC matrix $\mathbf{H}_{sc} = \mathbf{H}_{rep}(S,T) \circ \mathbf{W}$, whose null space gives an SC LDPC code over GF(2).

B. A general guideline for choosing the masking matrix and underlying block code

The R&M process gives the PC matrix $\mathbf{H}_{sc}$ of a resultant SC LDPC code that can be specified entirely by the LDPC block code PC matrix $\mathbf{H}$, and the parameters of the masking matrix $\mathbf{W}$. In this subsection, we analyze how the selection of masking matrix $\mathbf{W}$ and the PC matrix $\mathbf{H}$ affects the girth and periodicity property of the resultant SC PC matrix $\mathbf{H}_{sc}$.

In this paper, we mainly consider the construction of a SC LDPC code whose PC matrix is an array of permutation matrices and/or ZMs of the same size, say $Q \times Q$, which is of the greatest interest in practical application. In this case, as explained in Section III-A, the masking matrix is determined by the design target parameters of the SC code, including SC protograph and lifting size, etc. Given the masking matrix, the selection of the block code PC matrix $\mathbf{H}$ will determine the final PC matrix $\mathbf{H}_{sc}$ of the SC code. In the following lemmas, we show how the selection of $\mathbf{H}$ affects the girth and periodicity property [2].

[2]The proofs of the Lemmas and Theorems can be found in Appendix A.

This article has been accepted for publication in a future issue of this journal, but has not been fully edited. Content may change prior to final publication. Citation information: DOI 10.1109/JSAC.2015.2504273, IEEE Journal on Selected Areas in Communications

A(1,1)	A(1,2)	A(1,3)	A(1,4)	A(1,5)	A(1,6)	A(1,7)	A(1,8)	A(1,9)
A(2,1)	A(2,2)	A(2,3)	A(2,4)	A(2,5)	A(2,6)	A(2,7)	A(2,8)	A(2,9)
A(3,1)	A(3,2)	A(3,3)	A(3,4)	A(3,5)	A(3,6)	A(3,7)	A(3,8)	A(3,9)
A(4,1)	A(4,2)	A(4,3)	A(4,4)	A(4,5)	A(4,6)	A(4,7)	A(4,8)	A(4,9)

(a) The PC matrix $\mathbf{H}$ of an LDPC block code.

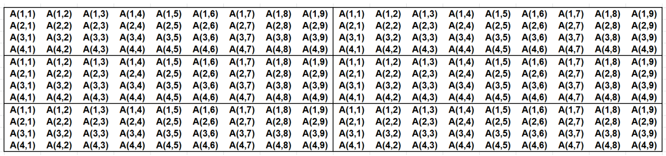

(b) The replication of $\mathbf{H}$ to form $\mathbf{H}_{rep}$

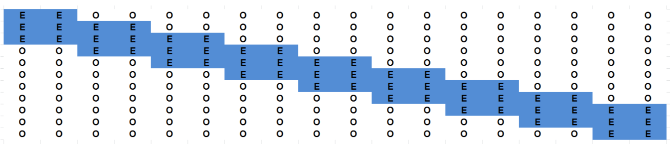

(c) The masking matrix $\mathbf{W}$ with a band-diagonal pattern.

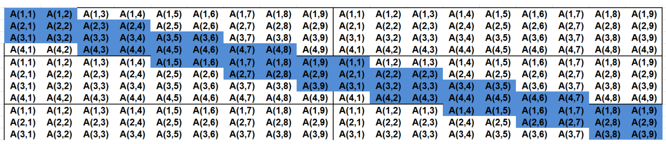

(d) The process of masking $\mathbf{H}_{rep}$ using $\mathbf{W}$

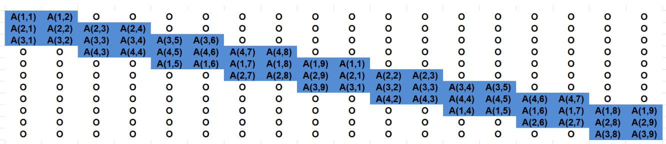

(e) The final PC matrix $\mathbf{H}_{sc}$ of the SC LDPC code after masking

Fig. 1. An Example of the R&M Construction of SC LDPC codes. Fig. 1(a) gives a PC matrix $\mathbf{H}$ of an LDPC block code, where $\{A(i,j)\}$ $(1 \le i \le 4, 1 \le j \le 9)$ is a set of permutation matrices of the same size, say $Q \times Q$. In Fig. 1(b), $\mathbf{H}$ is replicated to form a two-dimensional semi-infinite array $\mathbf{H}_{rep}$, where only the 3×2 subarray of $\mathbf{H}$ is shown. Fig. 1(c) shows the masking matrix $\mathbf{W}$ with a band-diagonal pattern, where E denotes a $Q \times Q$ all-one matrix and O denotes a $Q \times Q$ all-zero matrix (ZM). Therefore, $\mathbf{W}$ is an 11×18 band-diagonal array of $Q \times Q$ all-one matrices and/or all-zero matrices. Fig. 1(d) illustrates the process of masking $\mathbf{H}_{rep}$ with the masking matrix $\mathbf{W}$. Fig. 1(e) gives the PC matrix $\mathbf{H}_{sc}$ of the constructed SC LDPC code. Then, $\mathbf{H}_{sc}$ is an 11×18 band-diagonal array of $Q \times Q$ permutation matrices and/or zero matrices. It can be observed that $\mathbf{H}_{sc}$ is essentially the parity-check matrix of a $(3, 6, 9)$ protograph SC LDPC code with lifting size Q. If $Q = 3$, then Fig. 1(c) gives an example of the masking matrix $\mathbf{W}$ consisting of all-one binary component matrices $\{\Sigma_k\}$ $(0 \le k < 9)$, with parameters $A = 9, B = 6, C = 3, L = 9$.

Lemma 1: Let $\mathbf{W} = [w_{i,j}]_{0 \le i < S, 0 \le j < T}$ be the masking matrix used for the R&M construction, and let $\mathbf{H}$ be the $M \times N$ PC matrix of an LDPC block code used for the R&M construction. Suppose the girth of the Tanner graph of $\mathbf{H}$ is at least 6. For any i_1, i_2, j_1, j_2 with $0 \le i_1 < i_2 < S$, $0 \le j_1 < j_2 < T$ such that $w_{i_1,j_1} = w_{i_1,j_2} = w_{i_2,j_1} = w_{i_2,j_2} = 1$, if $i_1 - i_2$ is not divisible by M and $j_1 - j_2$ is not divisible by N, then the girth of the Tanner graph of $\mathbf{H}_{sc}$ is, also, at least 6.

In fact, if we slightly strengthen the condition given in Lemma 1, we have a stronger conclusion with respect to the girth property for $\mathbf{H}_{sc}$ as follows:

Lemma 2: Given a masking matrix $\mathbf{W}$, let $M_w(i) = \{j : w_{i,j} = 1\}$ and $N_w(j) = \{i : w_{i,j} = 1\}$, where $0 \le i < S$ and $0 \le j < T$. Suppose both of the following two conditions regarding the size of $\mathbf{H}$ are satisfied: (1) For any j and any $i_1, i_2 \in N_w(j)$, $i_1 - i_2$ is not divisible by M. (2) For any i and any $j_1, j_2 \in M_w(i)$, $j_1 - j_2$ is not divisible by N. Then, the girth of the Tanner graph of $\mathbf{H}_{sc}$ is at least as large as that of $\mathbf{H}$.

In general, the constructed SC LDPC codes using the R&M method is a terminated periodically time-varying SC LDPC codes. It is important to determine the periodicity of the SC LDPC codes since the periodicity is related to the implementation complexity. The following lemma specifies how the size of $\mathbf{H}$ determines the periodicity $\mathcal{T}$ of the constructed time-varying SC LDPC codes.

Lemma 3: Suppose a masking matrix $\mathbf{W}$ has a band-diagonal pattern and consists of L $A \times B$ binary component matrices $\{\Sigma_k\}$ $(0 \le k < L)$ with the 'step size' C, where $\Sigma_k = [\sigma_{i,j,k}]_{0 \le i < A, 0 \le j < B}$ for $0 \le k < L$, as defined in (3). Then, $\mathbf{H}_{sc}$ also consists of L $A \times B$ component matrices $\{\Psi_k\}$ $(0 \le k < L)$, corresponding to $\{\Sigma_k\}$ $(0 \le k < L)$, respectively, where $\Psi_k = [\psi_{i,j,k}]_{0 \le i < A, 0 \le j < B}$ and $\psi_{i,j,k} = \sigma_{i,j,k} \cdot h_{rep,i+kC,j+kB}$. Suppose all the binary component matrices are identical, i.e., $\Sigma_k = \Sigma' = \left[\sigma'_{i,j}\right]_{0 \le i < A, 0 \le j < B}$ $(0 \le k < L)$. Then, for $0 \le k_1 < k_2 < L$, we have $\Psi_{k_1} = \Psi_{k_2}$ if $k_2 - k_1 = \mathcal{T}$, where

$$\mathcal{T} = \frac{MN}{GCD(BM, CN)}.$$

Also, $\mathcal{T} = \frac{MN}{GCD(BM,CN)}$ is the smallest choice of $\mathcal{T}$ that can ensure that given M, N, A, B and C, $\Psi_k = \Psi_{k+\mathcal{T}}$ holds for any k [3], irrespective of the choice of $\mathbf{H}$ and Σ' .

For simplicity, we refer to $\mathcal{T}$ as the *block periodicity* for $\mathbf{H}_{sc}$.

Remark 1: Let the masking matrix $\mathbf{W}$ be constructed by the conventional unwrapping of an all-one matrix of the same size as $\mathbf{H}$. Then, $\mathbf{W}$ satisfies the conditions in both Lemma 1 and Lemma 2. Let $\mathbf{H}_{sc}$ be constructed by the R&M construction using $\mathbf{H}$ and $\mathbf{W}$. However, it is clear that $\mathbf{H}_{sc}$ can also be obtained by applying the same conventional unwrapping procedure to $\mathbf{H}$. Hence, *the conventional unwrapping is a* special case *of the R&M construction*. As will be illustrated in Section IV-B, the R&M construction has much more flexibility than the unwrapping construction in the selection of the PC matrix $\mathbf{H}$ of the underlying block code and the other parameters for optimizing the resultant SC LDPC code.

IV. The R&M Algebraic Construction of Binary SC QC LDPC Codes

The techniques presented in this section demonstrate a general algebraic construction of a very large class of SC QC LDPC codes on arbitrary finite fields.

The notation introduced in this section is summarized in Table II.

A. Algebraic construction of QC LDPC codes based on finite fields

Algebraic tools, such as finite fields, have been shown to be very effective in constructing QC LDPC codes with excellent

[3]Here we assume that L is sufficiently large and $\Psi_{k+\mathcal{T}}$ is well defined.

TABLE II
SUMMARY OF NOTATIONS USED IN SECTION IV

Notation	Explanation
$\mathbf{B}$,m,n,q,r	$\mathbf{B} = [b_{i,j}]_{0\leq i<m,0\leq j<n}$ is the $m \times n$ base matrix (over GF(q)) of the algebraic LDPC block code used in R&M algebraic construction described in Algorithm 2.
$\mathbf{H}_{qc}$	The $(q-1)$-fold dispersion of $\mathbf{B}$, which can also be viewed as the QC LDPC block code PC matrix used in the R&M construction described in Algorithm 1.
$\mathbf{W}_{base}$,s,t	$\mathbf{W}_{base} = [w_{base,i,j}]_{0\leq i<s,0\leq j<t}$ is the $s \times t$ masking matrix used in R&M algebraic construction described in Algorithm 2.
$\mathbf{B}_{sc}$	$\mathbf{B}_{sc} = [b_{sc,i,j}]_{0\leq i<s,0\leq j<t}$ is the base matrix of the constructed algebraic SC QC LDPC code.
$\mathbf{H}_{sc,qc}$	The PC matrix of constructed algebraic SC QC LDPC code, which is the $(q-1)$-fold dispersion of $\mathbf{B}_{sc}$.
$\{\Delta_k\}$, a, b, c, L	$\mathbf{W}_{base}$ typically consists of L $a \times b$ binary component matrices $\{\Delta_k\}$ ($0 \leq k < L$) with the 'step size' c, *cf.* (5).
$\mathbf{W}_{qc}$	The masking matrix used when constructing $\mathbf{H}_{sc,qc}$ with Algorithm 1 and the LDPC block code PC matrix $\mathbf{H}_{qc}$.

overall performance [13], [15], [23], [14], [29]. In most algebraic constructions of binary QC LDPC codes, the PC matrix of a code is an array of *circulant permutation matrices* (CPMs) and/or ZMs over GF(2). Consider a finite field GF(q) and let α be a primitive element of GF(q). The construction of a quasi-cyclic PC matrix $\mathbf{H}_{qc}$ starts with a matrix $\mathbf{B}$ over GF(q) (called *base matrix*). Given an $m \times n$ matrix $\mathbf{B} = [b_{i,j}]$ over GF(q), $\mathbf{H}_{qc}$ can be constructed directly from the base matrix $\mathbf{B}$ by a $(q-1)$-*fold dispersion* [13] of $\mathbf{B}$ as follows: for each entry $b_{i,j}$ in $\mathbf{B}$, if $b_{i,j} = 0$, then replace $b_{i,j}$ by the $(q-1) \times (q-1)$ ZM, otherwise let $b_{i,j} = \alpha^l$ with $0 \leq l < q-1$, then replace $b_{i,j}$ by an $(q-1) \times (q-1)$ CPM whose first row has a single 1-component at the l-th element.

It follows from the above construction process that $\mathbf{H}_{qc}$ is uniquely specified by the base matrix $\mathbf{B}$. It has been proved that a necessary and sufficient condition for the Tanner graph of $\mathbf{H}_{qc}$ to have a girth of at least 6 is that every 2×2 submatrix of $\mathbf{B}$ contains at least one zero entry or is non-singular [23]. This constraint on the 2×2 submatrices of $\mathbf{B}$ is referred to as the 2×2 *submatrix constraint* (SM-constraint). We call a matrix that satisfies the 2×2 SM-constraint over GF(q) a 2×2 *SM-constrained matrix*. Therefore, the construction of $\mathbf{H}_{qc}$ whose Tanner graph has a girth of at least 6 can be reduced to the construction of 2×2 SM-constrained base matrix $\mathbf{B}$ over GF(q). A detailed coverage of algebraic constructions of 2×2 SM-constrained base matrices can be found in [13], [15], [23], [14] and references therein.

B. A general R&M algebraic construction of SC QC LDPC codes

Suppose $\mathbf{B}$ is an $m \times n$ 2×2 SM-constrained matrix over GF(q). The $(q-1)$-fold dispersion of $\mathbf{B}$ results in an $m \times n$ array $\mathbf{H}_{qc}$ of $(q-1) \times (q-1)$ CPMs and/or ZMs. The null space of $\mathbf{H}_{qc}$ gives a QC LDPC block code whose Tanner graph has a girth of at least 6. As explained in Section III-A, if $\mathbf{H}_{qc}$ is chosen to be the PC matrix for the block code used in the R&M construction described in Algorithm 1, we can construct a binary matrix $\mathbf{W}_{qc} = [w_{qc,i,j}]_{0\leq i<s(q-1),0\leq j<t(q-1)}$ as the masking matrix, which is a $s \times t$ band diagonal array of $(q-1) \times (q-1)$ all-one matrices and/or ZMs, where s and t are two positive integers. Then, an SC QC LDPC PC matrix $\mathbf{H}_{sc,qc}$, which is a band-diagonal array of $(q-1)\times(q-1)$ CPMs and/or ZMs, can be constructed by applying the R&M method described in Algorithm 1 using the block code PC matrix $\mathbf{H}_{qc}$ and the masking matrix $\mathbf{W}_{qc}$. Since $\mathbf{H}_{qc}$ is constructed using the algebraic approach, the above process combines the R&M construction and the algebraic methods, which gives an algebraic construction of SC QC LDPC codes.

We can also observe another equivalent construction, which applies the R&M method on the base matrix. Note that $\mathbf{H}_{qc}$ can be completely specified by $\mathbf{B}$. Consider a masking matrix $\mathbf{W}_{base}$ obtained by replacing each $(q-1) \times (q-1)$ all-one matrix and each ZM in $\mathbf{W}_{qc}$ by 1 and 0, respectively. Firstly, we can perform the R&M process with the block code base matrix $\mathbf{B}$ and masking matrix $\mathbf{W}_{base}$. This results in a band-diagonal base matrix $\mathbf{B}_{sc}$ over GF(q). Then, we can apply the $(q-1)$-fold dispersion on $\mathbf{B}_{sc}$ which gives exactly the same SC QC LDPC PC matrix $\mathbf{H}_{sc,qc}$ as mentioned above. To summarize, an equivalent R&M algebraic construction of SC QC LDPC codes is presented in Algorithm 2.

Algorithm 2 R&M algebraic construction of SC QC LDPC codes

1: Construct a 2×2 SM-constrained base matrix $\mathbf{B} = [b_{i,j}]_{0\leq i<m,0\leq j<n}$ over GF(q).
2: Replicate $\mathbf{B}$ to form a two-dimensional semi-infinite array $\mathbf{B}_{rep}$ of $\mathbf{B}$ as follows:
$$\mathbf{B}_{rep} = [b_{rep,i,j}]_{0\leq i,j<\infty} = \begin{bmatrix} \mathbf{B} & \mathbf{B} & \mathbf{B} & \cdots \\ \mathbf{B} & \mathbf{B} & \mathbf{B} & \cdots \\ \mathbf{B} & \mathbf{B} & \mathbf{B} & \cdots \\ \vdots & \vdots & \vdots & \ddots \end{bmatrix}, \quad (4)$$
where $b_{rep,i,j} = b_{(i \mod m),(j \mod n)}$ for all $i,j \geq 0$.
3: Design an $s \times t$ masking matrix $\mathbf{W}_{base} = [w_{base,i,j}]_{0\leq i<s,0\leq j<t}$ with a desired band-diagonal pattern.
4: Take an $s \times t$ submatrix $\mathbf{B}(s,t)$ of $\mathbf{B}$, from the upper left corner of $\mathbf{B}_{rep}$.
5: Mask $\mathbf{B}_{rep}(s,t)$ using $\mathbf{W}_{base}$ to obtain an SC base matrix $\mathbf{B}_{sc} = \mathbf{B}_{rep}(s,t) \circ \mathbf{W}_{base}$.
6: Apply $(q-1)$-fold dispersion on $\mathbf{B}_{sc}$ to obtain an $s \times t$ SC QC array $\mathbf{H}_{sc,qc}$ of $(q-1) \times (q-1)$ CPMs and/or ZMs, whose null space gives a binary SC QC LDPC code.

Remark 2: Constructing $\mathbf{H}_{sc,qc}$ using Algorithm 2 is equivalent to implementing Algorithm 1 where $\mathbf{H}_{qc}$ is chosen as $\mathbf{H}$

in Step 1 and $\mathbf{W}_{qc}$ is chosen as $\mathbf{W}$ in Step 3. In this case, the notations between two algorithms have the the following relationships: $S = s(q-1)$, $T = t(q-1)$, $M = m(q-1)$, and $N = n(q-1)$.

Remark 3: In the terminologies of protograph construction [27], it is clear that the masking matrix $\mathbf{W}_{base}$ can be viewed as the protomatrix corresponding to the SC protograph (with no more than 1 edge between each pair of VN and CN). Also, the above construction is equivalent to lifting the SC protograph corresponding to $\mathbf{W}_{base}$ with lifting size $q-1$, however, the lifting (the permutation of the edges) is carried out using an algebraic approach. More generally, this construction can be considered as a superposition construction [31], [32] of SC LDPC codes, and the base matrix for superposition is exactly the same as the masking matrix $\mathbf{W}_{base}$.

Given $\mathbf{W}_{base}$, it is clear that the final R&M SC QC LDPC PC matrix $\mathbf{H}_{sc,qc}$ depends totally on the selection of $\mathbf{B}$. Following the lemmas in Section III, we readily obtain some conclusions on how the selection of $\mathbf{B}$ affect the periodicity of the time-varying and the girth properties.

Theorem 1, below, is a direct consequence of Lemma 1 for algebraic QC LDPC codes.

Theorem 1: Suppose $\mathbf{B}_{sc} = \mathbf{B}_{rep}(s,t) \circ \mathbf{W}_{base}$ and $\mathbf{B}$ is an $m \times n$ matrix over GF(q) satisfying the 2×2 SM-constraint. Then, $\mathbf{B}_{sc}$ also satisfies the 2×2 SM-constraint if the following condition regarding the size of $\mathbf{B}$ is satisfied: $i_1 - i_2$ is not divisible by m and $j_1 - j_2$ is not divisible by n, for any i_1, i_2, j_1, j_2 such that $w_{base,i_1,j_1} = w_{base,i_1,j_2} = w_{base,i_2,j_1} = w_{base,i_2,j_2} = 1$,

As is the case for the masking matrix $\mathbf{W}$ in the general R&M method described in Algorithm 1, typically, the masking matrix $\mathbf{W}_{qc}$ with a band-diagonal pattern also consists of L $A \times B$ binary component matrices $\{\Sigma_k\}$ $(0 \le k < L)$ with the 'step size' C, as described in Section III-B. In this case, each of the binary component matrices $\{\Sigma_k\}$ is typically an $a \times b$ array of $(q-1)\times(q-1)$ all-one matrices and/or ZMs. Based on this fact, $\mathbf{W}_{base}$ typically consists of L $a \times b$ binary component matrices $\{\Delta_k\}$ $(0 \le k < L)$ with the 'step size' $c = C/(q-1)$, where $\Delta_k = [\delta_{i,j,k}]_{0 \le i < a, 0 \le j < b}$ $(0 \le k < L)$ is obtained by replacing each $(q-1)\times(q-1)$ all-one matrix and each ZM in Δ_k by 1 and 0, respectively. In this case, $s = cL + (a-c)$, $t = bL$, and $\mathbf{W}_{base} = [w_{base,i,j}]_{0 \le i < (cL+(a-c)), 0 \le j < bL}$, where for $\mathcal{I} \equiv (kc \le i < kc + a) \& (kb \le j < (k+1)b)$ for $0 \le k < L$,

$$w_{base,i,j} = \begin{cases} \delta_{i-kc,j-kb,k} & \text{if } \mathcal{I}, \\ 0 & \text{otherwise.} \end{cases} \tag{5}$$

Fig. 2 gives an example of the masking matrix $\mathbf{W}_{base}(a,b,c,L)$.

Following from Theorem 1, the following two theorems give a general guideline on how to choose the size of $\mathbf{B}$, given $\mathbf{W}_{base}$ in the form given by (5).

Theorem 2: Suppose $\mathbf{B}$ satisfies the 2×2 SM-constraint. Then, $\mathbf{B}_{sc}$ is a 2×2 SM-constrained masked matrix, if $a \le m$ and $\lceil (a-1)/c \rceil b \le n$ for the masking matrix $\mathbf{W}_{base}$.

The following Theorem 3 is a direct consequence of Lemma 2.

Theorem 3: Suppose $\mathbf{H}_{qc}$ is the $(q-1)$-fold dispersion of $\mathbf{B}$. If $a \le m$ and $\lceil a/c \rceil b \le n$, the girth of the Tanner graph of $\mathbf{H}_{sc,qc}$ is at least as large as that of the Tanner graph of $\mathbf{H}_{qc}$.

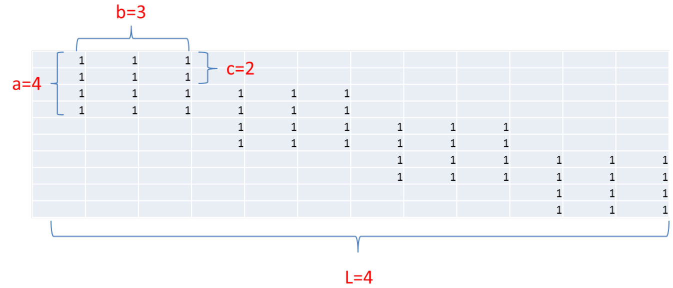

Fig. 2. An example of $\mathbf{W}_{base}$ where $a = 4, b = 3, c = 2, L = 4$, and all the 4 binary component matrices $\{\Delta_k\}$ $(0 \le k < 4)$ are all-one matrices.

As described in Section III-B, $\mathbf{H}_{sc,qc}$ also consists of L $A \times B$ component matrices $\{\Psi_k\}$ $(0 \le k < L)$, corresponding to $\{\Sigma_k\}(0 \le k < L)$, respectively. Each of the component matrices $\{\Psi_k\}$ $(0 \le k < L)$ is an $a \times b$ array of $(q-1)\times(q-1)$ CPMs and/or ZMs. It follows from Lemma 3 that its block periodicity $\mathcal{T}_{qc}$ of $\mathbf{H}_{sc,qc}$ is

$$\mathcal{T}_{qc} = \frac{mn}{GCD(bm, cn)}. \tag{6}$$

Note that if the constructed SC QC PC array $\mathbf{H}_{sc,qc}$ has full row rank, the rate of the SC QC LDPC codes constructed based on $\mathbf{W}_{base}$ is $1 - (cL + a - c)/bL = (b-c)/b - (a-c)/bL$, where $(b-c)/b$ is the designed rate, and $(a-c)/bL$ is the rate loss due to the edge effect. Also, the length of the constructed SC QC LDPC codes is $bL(q-1)$.

Fig. 3 gives three examples of the R&M construction of (3,6)-regular SC base matrices $\mathbf{B}_{sc}$, all of which satisfy the condition in Theorem 2. It illustrates that for given masking matrix $\mathbf{W}_{base}$, the number of entries in $\mathbf{B}$ can represent the degree of freedom in optimizing the constructed $\mathbf{H}_{sc,qc}$. This also verifies the claim of Remark 1 that the R&M construction can provide larger degrees of freedom and more flexibility in the parameter selection than the unwrapping construction.

C. Rank analysis of the SC PC matrices

The rank of QC LDPC codes can be analysed by expressing the Galois field Fourier transform of a QC array in terms of the Hadamard powers of its base matrix [23]. In the following, we analyze the rank of the SC QC array $\mathbf{H}_{sc,qc}$, for the case in which the following three conditions are satisfied: (1) $q = 2^r$ is a power of 2; (2) all elements of the base matrix $\mathbf{B}$ are non-zero; and (3) all the L binary component matrices $\{\Delta_k\}$ $(0 \le k < L)$ are all-one matrices. Let $\mathbf{B}^{\circ t}$ denote the tth Hadamard power of $\mathbf{B}$, which is the Hadamard product of t copies of $\mathbf{B}$. With the Fourier transform analysis, it follows that the rank of $\mathbf{H}_{sc,qc}$ is given by the sum of the ranks of the base matrix $\mathbf{B}_{sc}$ and its Hadamard powers, i.e. for $q = 2^r$,

$$\text{rank}(\mathbf{H}_{sc,qc}) = \sum_{t=0}^{2^r-2} \text{rank}(\mathbf{B}_{sc}^{\circ t}). \tag{7}$$

Then, with (7), an upper bound on $\text{rank}(\mathbf{H}_{sc,qc})$ can be specified, as in Theorem 4.

Theorem 4: The rank of $\mathbf{H}_{sc,qc}$ is upper bounded by $(cL + a - c)(q-1) - ((c-1)L + a - c)$.

This article has been accepted for publication in a future issue of this journal, but has not been fully edited. Content may change prior to final publication. Citation information: DOI 10.1109/JSAC.2015.2504273, IEEE Journal on Selected Areas in Communications

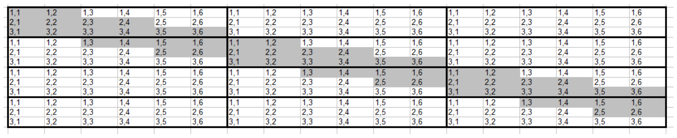

(a) $m = 3, n = 6, a = 3, b = 2$, and $c = 1$.

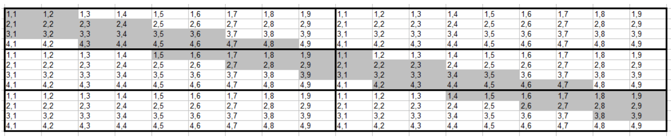

(b) $m = 4, n = 9, a = 3, b = 2$, and $c = 1$

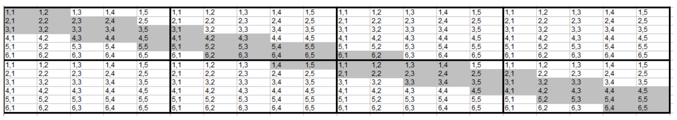

(c) $m = 6, n = 5, a = 3, b = 2$, and $c = 1$

Fig. 3. Examples of constructing algebraic (3,6)-regular SC QC LDPC codes using Algorithm 2. Fig. 3(a) results in an unwrapping construction, where the base matrix $\mathbf{B}$ of the QC LDPC block code has 18 entries. Whereas the conventional unwrapping construction of (3,6)-regular SC LDPC codes must start with a (3,6)-regular LDPC block code with a base matrix of 18 entries, the number of entries in the base matrices of the QC LDPC block codes in Fig. 3(b) and 3(c) are 36 and 30, respectively. Fig. 3(c) also gives an example of constructing R&M SC LDPC codes with constraint length greater than the length of the underlying LDPC block codes, which can not be done by the conventional unwrapping construction.

Next, we consider a special case. Suppose $a = m$ and $\mathbf{B}$ is rank-deficient (This is usually true for most of the algebraic constructions [23], [15]). Let $\mathbf{b}_0, \mathbf{b}_1, ..., \mathbf{b}_{m-1}$ denote the m rows in $\mathbf{B}$. Then, there exist m elements in GF(q) among which at least one element is non-zero, denoted by $k_0, k_1, ..., k_{m-1}$, such that $\sum_{i=0}^{m-1} k_i \mathbf{b}_i = \mathbf{0}$. For $0 \leq i < cL+(a-c)$, we define $p_i = k_{i \bmod m}$. Let $\mathbf{b}_{sc,0}, \mathbf{b}_{sc,1}, ..., \mathbf{b}_{sc,cL+(a-c)-1}$ denote all the $cL + (a - c)$ rows in $\mathbf{B}_{sc}$, respectively. Then, we can verify that $\sum_{i=0}^{cL+(a-c)-1} p_i \mathbf{b}_{sc,i} = \mathbf{0}$, which implies that $\mathbf{B}_{sc}$ is also rank-deficient and has at least 1 redundant row. Since GF(q) has a characteristic 2 [33], we have $\mathrm{rank}(\mathbf{B}_{sc}^{\circ 1}) = \mathrm{rank}(\mathbf{B}_{sc}^{\circ 2}) = \mathrm{rank}(\mathbf{B}_{sc}^{\circ 2^2}) = ... = \mathrm{rank}(\mathbf{B}_{sc}^{\circ 2^{r-1}})$. Hence, in this case, $\mathbf{H}_{sc,qc}$ has at least r additional redundant rows. Together with Theorem 4, we have the following theorem.

Theorem 5: If $a = m$ and $\mathbf{B}$ does not have full row rank, the rank of $\mathbf{H}_{sc,qc}$ is upper bounded by $(cL+a-c)(q-1)-((c-1)L+a-c+r)$.

It is shown in Example 1 of the following section that the bound of Theorem 5 is tight in many cases.

V. Examples of R&M Algebraic SC QC LDPC Codes

In this section, we use several examples to illustrate the proposed algebraic constructions of various types of SC QC LDPC codes, including the regular, irregular and rate compatible SC QC LDPC codes, and show the performance of the constructed codes using the FSD. In this section, it will be demonstrated that the finite-length R&M SC LDPC codes can have better error rate performance than the corresponding unwrapped SC LDPC codes, and block LDPC codes.

Although Sections III and IV focus on the construction of binary SC LDPC codes, we would like to point out that the non-binary SC LDPC codes can also be constructed using the R&M construction. Specifically, suppose we would like to construct a R&M SC QC LDPC code over GF(2^p). First, we use the R&M method in Algorithm 2 to construct a binary SC QC PC matrix $\mathbf{H}_{sc,qc}$. Then, we apply a simple binary to non-binary (B-to-NB) replacement procedure [34] which is carried out as follows: for each CPM of size $(q-1) \times (q-1)$, we replace all the 1-entries in the CPM by a non-zero element in GF(2^p). After such B-to-NB replacement, we obtain a SC QC PC matrix $\mathbf{H}_{sc,qc,nb}$ over GF(2^p), whose null space gives an SC QC LDPC code over GF(2^p). In the B-to-NB replacement, the non-zero element from GF(2^p) can be chosen either randomly or in a systematic way, as will be shown later in the examples.

It is worth noting that the block periodicity given by (6) is for the binary SC QC PC matrix $\mathbf{H}_{sc,qc}$. For the SC QC LDPC codes over GF(2^p), the block periodicity $\mathcal{T}_{nb}$ will depend on the specific B-to-NB replacement. In particular, the $\mathbf{H}_{sc,qc,nb}$ will be completely non-periodically time-varying if a completely random B-to-NB replacement is performed.

Suppose the constructed code is over GF(2^p). For simplicity, we assume BPSK transmission over the AWGN channel, where each symbol in GF(2^p) is expanded into p bits for BPSK transmission. All the simulations, in this section, are performed using the sum-product algorithm (SPA), i.e the Fast Fourier Transform (FFT) q-ary sum-product decoding algorithm [13] for non-binary codes, with the maximum number of iterations set to 1000. Based on the R&M construction procedure proposed in Section IV, it is sufficient to specify the 2×2 SM-constrained matrix $\mathbf{B}$, the SC masking matrix $\mathbf{W}_{base}$, and the assignment of nonzero elements over GF(2^p) for the non-binary code construction.

A. Non-binary Regular SC QC LDPC Code Construction

Example 1: A Regular R&M SC QC LDPC code over GF(2^2)

Selection of $\mathbf{B}$: Suppose the 2×2 SM-constrained matrix $\mathbf{B}$ is constructed using GF(q) where $q = 2^r$. We choose $r = 7$, $m = 3$ and $n = 64$. Consider the following 2×2 SM-constrained matrix $\mathbf{B}$ over GF(2^7) constructed using the method proposed in [35],

$$\mathbf{B} = \begin{bmatrix} \alpha^{63} & \alpha^{64} & \cdots & \alpha^{125} \\ 1+\alpha^{63} & 1+\alpha^{64} & \cdots & 1+\alpha^{125} \\ \alpha+\alpha^{63} & \alpha+\alpha^{64} & \cdots & \alpha+\alpha^{125} \end{bmatrix}. \tag{8}$$

Selection of $\mathbf{W}_{base}$: We construct a masking matrix, which is the protomatrix of the SC protograph $\mathcal{C}_{[3,6]}^{m_s=2}$ in Page 2 defined in [25]. Specifically, we choose $L = 40, a = 3, b = 2, c = 1$, and choose all the 40 component regular matrices $\{\Delta_k\}$ $(0 \leq k < 40)$ to be all-one matrices. Then, the masking matrix $\mathbf{W}_{base}$ is constructed based on (5).

R&M process: Using the R&M process given in Algorithm 2, we obtain a 42×80 SC array $\mathbf{H}_{sc,qc}$ of 127×127 CPMs and ZMs.

Assignment of non-zero elements from GF(2^2): Label the columns of CPMs and ZMs from 0 to 79. Then, for $0 \leq i < 80$, we replace all the 1-entries in the i-th column of CPMs and ZMs in $\mathbf{H}_{sc,qc}$ by β^i, where β is a primitive element of GF(2^2). After such replacement procedure, we obtain a 42×80

This article has been accepted for publication in a future issue of this journal, but has not been fully edited. Content may change prior to final publication. Citation information: DOI 10.1109/JSAC.2015.2504273, IEEE Journal on Selected Areas in Communications

SC array $\mathbf{H}_{sc,qc,nb}$ of 127×127 *weighted* CPMs and ZMs, which is a 5334×10160 matrix over GF(2^2). Note that the block periodicity of $\mathbf{H}_{sc,qc}$ is 96 based on (6), which is larger than 40. Therefore, both $\mathbf{H}_{sc,qc,nb}$ and $\mathbf{H}_{sc,qc}$ are essentially non-periodically time-varying SC QC LDPC codes due to the termination.

We find that the rank of $\mathbf{H}_{sc,qc,nb}$ is equal to 5325. Note that $\mathbf{H}_{sc,qc,nb}$ is obtained by performing elementary column operations on $\mathbf{H}_{sc,qc}$. Hence, the upper bound on the rank of $\mathbf{H}_{sc,qc}$ given by Theorem 5 is tight in this example. Thus, the null space of $\mathbf{H}_{sc,qc,nb}$ gives an (10160,4835) SC QC LDPC codes over GF(2^2), denoted by $\mathcal{C}_{sc,qc}$, with rate 0.4759.

The symbol and block error performances of $\mathcal{C}_{sc,qc}$ are shown in Fig. 4 with the legend "algebraic R&M SCQC". For comparison, also included in Fig. 4, are the error performances of two (10160,4826) LDPC block codes over GF(2^2) with rate 0.4750, the first is constructed algebraically based on a Latin square over GF(2^7) [15] and labeled "algebraic block", and the second is constructed using the progressive edge growth (PEG) algorithm [18] with random non-zero entry assignments and labeled "PEG block". Both of them have constant column weight 3, and the same PC matrix size as $\mathbf{H}_{sc,qc}$. The operating block error rate (BLER) of many cellular wireless communication systems (e.g. 3GPP LTE) is around 10^{-2}. At BLER of 10^{-2}, the R&M SC QC LDPC code $\mathcal{C}_{sc,qc}$ has a coding gain of about 0.13-0.14 dB over these two block codes . The error performances are also compared to that of an (10160, 4826) SC LDPC code over GF(2^2) constructed by the conventional step-shape unwrapping of the PC matrix of an (762,381) (3,6)-regular PEG LDPC block code, and labeled "SC PEG unwrap". The PC matrix $\mathbf{H}_{sc,PEG}$ of this SC LDPC code has the same size and almost the same degree distributions as $\mathbf{H}_{sc,qc,nb}$. For fair comparison, the assignment of the non-zero values from GF(2^2) on the $\mathbf{H}_{sc,PEG}$ is made such that $\mathbf{H}_{sc,PEG}$ is also non-periodically time-varying. It is shown that at the BLER of 10^{-2}, the proposed algebraic R&M SC QC LDPC code $\mathcal{C}_{sc,qc}$ has about 0.15 dB coding gain over the corresponding SC LDPC code constructed by unwrapping a PEG block code. It is also observed that the constructed codes do not suffer from error floors.

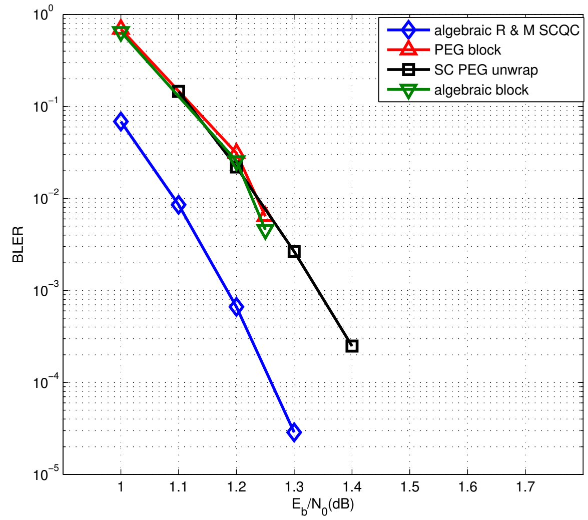

(a) BLER

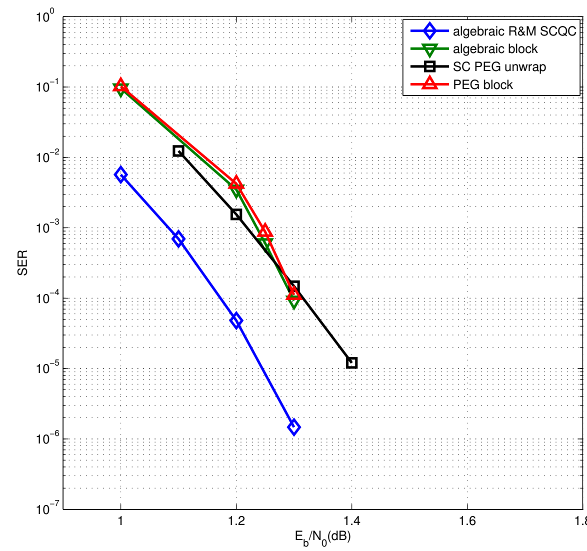

(b) SER

Fig. 4. BI-AWGNC error performances of the proposed algebraic R&M SC QC LDPC codes compared to other SC codes and block codes, given in Example 1.

B. Irregular SC QC LDPC Code Construction

In this subsection, we consider the R&M construction of irregular SC QC LDPC codes. To our best knowledge, constructions of such codes have not been addressed in the literature before.

Example 2: Construction of an irregular binary SC QC LDPC code.

Selection of B: Consider the following 2×2 SM-constrained matrix $\mathbf{B}$ over GF(2^7), constructed based on a Latin square [15] over GF(2^7):

$$\mathbf{B} = \begin{bmatrix} \alpha^{63} & \alpha^{64} & \cdots & \alpha^{126} \\ 1+\alpha^{63} & 1+\alpha^{64} & \cdots & 1+\alpha^{126} \\ \vdots & \vdots & \ddots & \vdots \\ \alpha^{62}+\alpha^{63} & \alpha^{62}+\alpha^{64} & \cdots & \alpha^{62}+\alpha^{126} \end{bmatrix}, \tag{9}$$

where α is a primitive element in GF(2^7).

Construction of the masking matrix $\mathbf{W}_{base}$: We consider a rate 1/3 protograph of a structured irregular LDPC code in Fig. 5(a), constructed by El-Khamy et al. [36] from ARCA codes [37]. The corresponding protomatrix is as follows:

$$\mathbf{V} = \begin{bmatrix} 1&1&1&1&0&0&0&0 \\ 0&1&1&0&0&0&0&0 \\ 0&1&1&0&1&0&0&0 \\ 0&1&1&1&0&1&0&0 \\ 0&1&0&1&1&0&1&1 \\ 0&0&1&1&0&1&1&1 \end{bmatrix}. \tag{10}$$

In order to preserve the degree distribution of the original irregular structured block code, we construct the base masking matrix $\mathbf{W}_{base}$ by *unwrapping* $\mathbf{V}$. We decompose $\mathbf{V}$ into two matrices $\mathbf{V}_0$ and $\mathbf{V}_1$ such that $\mathbf{V} = \mathbf{V}_0 + \mathbf{V}_1$ (summation over

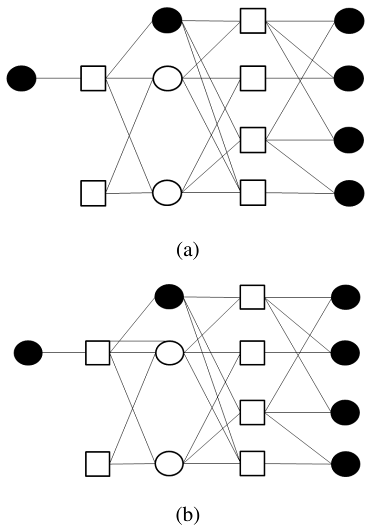

Fig. 5. Irregular SC QC LDPC codes will be constructed based on above protographs proposed in [36]. White variable nodes are punctured.

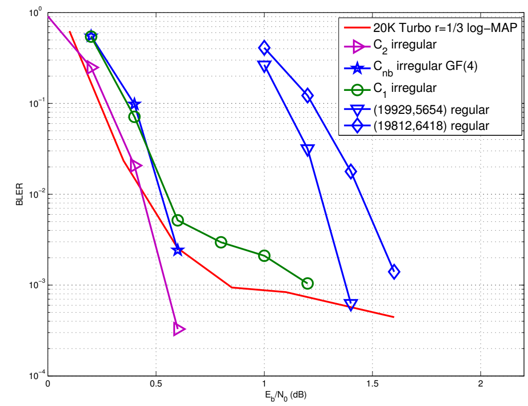

Fig. 6. BLER performances of rate 1/3, length 20,000 bits code are compared on BI-AWGNC. Proposed irregular punctured binary and non-binary R&M SC QC LDPC codes are better than the corresponding regular SC LPDC codes, and also better than turbo codes at the error floor region.

integer ring), where

$$\mathbf{V}_0 = \begin{bmatrix} 1 & 0 & 1 & 0 & 0 & 0 & 0 & 0 \\ 0 & 1 & 0 & 0 & 0 & 0 & 0 & 0 \\ 0 & 1 & 0 & 0 & 1 & 0 & 0 & 0 \\ 0 & 1 & 0 & 1 & 0 & 0 & 0 & 0 \\ 0 & 1 & 0 & 0 & 1 & 0 & 1 & 0 \\ 0 & 0 & 1 & 0 & 0 & 1 & 0 & 1 \end{bmatrix},$$

$$\mathbf{V}_1 = \begin{bmatrix} 0 & 1 & 0 & 1 & 0 & 0 & 0 & 0 \\ 0 & 0 & 1 & 0 & 0 & 0 & 0 & 0 \\ 0 & 0 & 1 & 0 & 0 & 0 & 0 & 0 \\ 0 & 0 & 1 & 0 & 0 & 1 & 0 & 0 \\ 0 & 0 & 0 & 1 & 0 & 0 & 0 & 1 \\ 0 & 0 & 0 & 1 & 0 & 0 & 1 & 0 \end{bmatrix}. \tag{11}$$

Choosing $L = 26$, we obtain the following 162×208 masking matrix $\mathbf{W}_{base}$, which is a 27×26 array $\mathbf{B}_{sc}$ of 6×8 matrices:

$$\mathbf{W}_{base} = \begin{bmatrix} \mathbf{V}_0 & & & & & \\ \mathbf{V}_1 & \mathbf{V}_0 & & & & \\ & \mathbf{V}_1 & \mathbf{V}_0 & & & \\ & & \mathbf{V}_1 & & & \\ & & & \ddots & \ddots & \mathbf{V}_0 \\ & & & & & \mathbf{V}_1 \end{bmatrix}. \tag{12}$$

We can readily verify that the base matrix $\mathbf{B}$ and the masking matrix $\mathbf{W}_{base}$ satisfy the conditions in Theorem 1. Therefore, we construct the final SC QC PC matrix $\mathbf{H}_{sc,qc}$ using the R&M approach proposed in Algorithm 2. The resulting code is a punctured (19812,5969) binary SC QC LDPC code, denoted by C_1.

Also, we can construct a corresponding non-binary irregular SC QC LDPC code over GF(2^2) with similar code length (in bits), which is illustrated in the following example.

Example 3: Construction of an irregular non-binary SC QC LDPC code.
Selection of B: We consider the following matrix $\mathbf{B}$ over GF(2^6), which is constructed based on a Latin square over GF(2^6) [15]:

$$\mathbf{B} = \begin{bmatrix} \beta^{31} & \beta^{32} & \cdots & \beta^{62} \\ 1+\beta^{31} & 1+\beta^{32} & \cdots & 1+\beta^{62} \\ \vdots & \vdots & \ddots & \vdots \\ \beta^{30}+\beta^{31} & \beta^{30}+\beta^{32} & \cdots & \beta^{30}+\beta^{62} \end{bmatrix}, \tag{13}$$

where β is a primitive element in GF(2^6).
Construction of the masking matrix $\mathbf{W}_{base}$: Same masking matrix $\mathbf{W}_{base}$ as Example 2.
Assignment of non-zero elements from GF(2^2): For each column of CPMs/ZMs in $\mathbf{H}_{sc,qc}$, choose a nonzero element randomly from GF(2^2) and replace all the 1-components in this column of CPMs/ZMs by this nonzero element. After such random replacement procedure, we obtain a non-binary SC QC PC array $\mathbf{H}_{sc,qc,nb}$, corresponding to a punctured (9828,2961) SC QC LDPC code over GF(2^2), denoted by C_{nb}.

QC LDPC block codes constructed by two-stage protograph lifting can have better minimum distance properties than those constructed by a one-stage lifting [38]. Hence, Example 4 illustrates another new construction of irregular SC QC LDPC codes which deploys two-stage graph lifting.

Example 4: A two-stage lifting construction of an irregular SC QC LDPC code
Selection of B: Same as in Example 3.
Design of $\mathbf{W}_{base}$ by two-stage lifting: We consider a variation of the protograph in Fig. 5(a), which is shown in Fig. 5(b) and also proposed in [36]. Compared to the protograph in Fig. 5(a), this protograph has multiple edges. Its corresponding protomatrix is as follows

$$\mathbf{V}^* = \begin{bmatrix} 1 & 2 & 1 & 1 & 0 & 0 & 0 & 0 \\ 0 & 1 & 1 & 0 & 0 & 0 & 0 & 0 \\ 0 & 1 & 1 & 0 & 1 & 0 & 0 & 0 \\ 0 & 1 & 1 & 1 & 0 & 1 & 0 & 0 \\ 0 & 1 & 0 & 1 & 1 & 0 & 1 & 1 \\ 0 & 0 & 1 & 1 & 0 & 1 & 1 & 1 \end{bmatrix}. \tag{14}$$

The multi-edge protograph will be decomposed into a sum of binary matrices over integer ring. For this example, $\mathbf{V}^*$ is decomposed into $\mathbf{V}_0^*$ and $\mathbf{V}_1^*$, such that $\mathbf{V}^* = \mathbf{V}_0^* + \mathbf{V}_1^*$:

$$\mathbf{V}_0^* = \begin{bmatrix} 1 & 1 & 1 & 0 & 0 & 0 & 0 & 0 \\ 0 & 1 & 0 & 0 & 0 & 0 & 0 & 0 \\ 0 & 1 & 0 & 0 & 1 & 0 & 0 & 0 \\ 0 & 1 & 0 & 1 & 0 & 0 & 0 & 0 \\ 0 & 1 & 0 & 0 & 1 & 0 & 1 & 0 \\ 0 & 0 & 1 & 0 & 0 & 1 & 0 & 1 \end{bmatrix},$$

This article has been accepted for publication in a future issue of this journal, but has not been fully edited. Content may change prior to final publication. Citation information: DOI 10.1109/JSAC.2015.2504273, IEEE Journal on Selected Areas in Communications

$$\mathbf{V}_1^* = \begin{bmatrix} 0 & 1 & 0 & 1 & 0 & 0 & 0 & 0 \\ 0 & 0 & 1 & 0 & 0 & 0 & 0 & 0 \\ 0 & 0 & 1 & 0 & 0 & 0 & 0 & 0 \\ 0 & 0 & 1 & 0 & 0 & 1 & 0 & 0 \\ 0 & 0 & 0 & 1 & 0 & 0 & 0 & 1 \\ 0 & 0 & 0 & 1 & 0 & 0 & 1 & 0 \end{bmatrix}. \quad (15)$$

Using the unwrapping technique with $L = 26$, we obtain the following 27×26 array $\mathbf{W}^*_{base}$ of 6×8 matrices, which is an 162×208 matrix:

$$\mathbf{W}^*_{base} = \begin{bmatrix} \mathbf{V}_0^* & & & & \\ \mathbf{V}_1^* & \mathbf{V}_0^* & & & \\ & \mathbf{V}_1^* & \mathbf{V}_0^* & & \\ & & \mathbf{V}_1^* & & \\ & & & \ddots & \ddots & \mathbf{V}_0^* \\ & & & & & \mathbf{V}_1^* \end{bmatrix}. \quad (16)$$

In each column of matrices in $\mathbf{W}^*_{base}$, the second and third variable nodes (columns) are punctured for a designed rate of 1/3.

Replacing each 1-entry in $\mathbf{W}^*_{base}$ by a 2×2 permutation matrix chosen randomly, we obtain a 324×416 matrix $\mathbf{W}_{base}$, whose corresponding protograph can be obtained by pre-lifting the protograph of $\mathbf{W}^*_{base}$ with a lifting size 2. $\mathbf{W}_{base}$ will be the masking matrix used in the R&M construction.

Since Theorem 1 is satisfied, the R&M construction is deployed to construct a binary SC QC PC array $\mathbf{H}_{sc,qc}$. The resulting code is a (19656,5922) binary SC QC LDPC code, denoted by C_2.

Fig. 6 gives the BLER performance of the three irregular SC QC LDPC codes of Examples 2-4 on the BI-AWGNC. Their performances are also compared with that of the 1/3 rate 3GPP turbo code with a random interleaver. To show the performance superiority of the irregular SC QC LDPC codes, the error performances are also compared with those of two near-regular SC QC LDPC codes of similar block lengths, constructed also using R&M approach. We see that the proposed punctured irregular R&M SC QC LDPC codes are better than the near-regular SC QC LDPC codes by 0.6-0.8 dB. The advantage of a non-binary construction is illustrated at the error floor region, where the non-binary code is superior to the binary code constructed from the same protograph. The two-stage lifted binary SC QC code C_2 has the best performance among the compared LDPC codes. The performances of the three irregular SC QC LDPC codes are also compared to that of 3GPP turbo codes used in the HSPA and LTE celluar wireless system. It comparable to the turbo code at the waterfall region, and is more superior to turbo codes at the error floor region.

C. Rate-Compatible Irregular SC QC LDPC codes

This subsection addresses the construction of rate-compatible (RC) structured SC LDPC codes suitable for incremental redundancy HARQ applications. The construction of rate-compatible LDPC codes for HARQ applications has been studied (*cf.* [36] and references therein) and that of RC SC LDPC codes has been recently addressed [39], [40]. In this subsection, we investigate the performance of RC algebraic SC QC LDPC codes of practical length (say 6k information block length in bits) constructed based on finite fields.

It is worth noting that punctured LDPC codes, to be transmitted on AWGN channels, must have good performance on

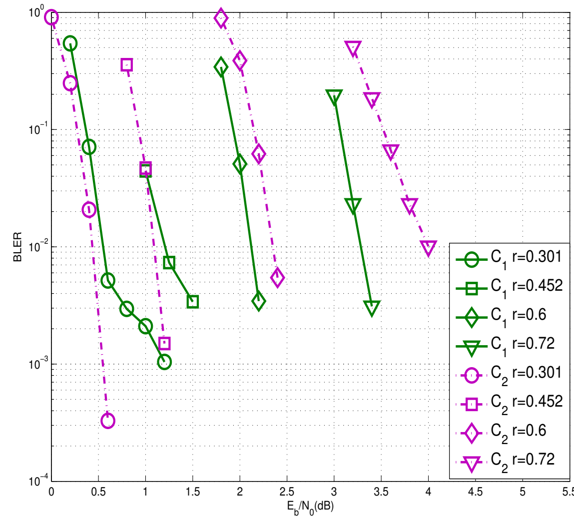

(a) BLER

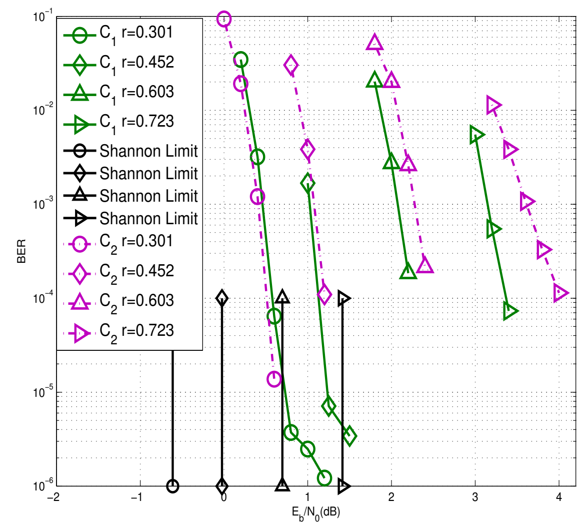

(b) BER

Fig. 7. The performance of the binary RC R&M SC QC LDPC codes with information length of 6k (in bits) and regular puncturing pattern in Table III.

both the AWGN and erasure channel. One of our motivations to construct structured SC LDPC codes is to benefit from the universality property of SC LDPC codes, where SC codes universally achieve the capacity of general BMS channels under belief propagation decoding [41]. Hence, RC families of SC LDPC codes obtained by puncturing mother codes are expected to be capacity achieving. Also, the girth properties enforced by the QC structure and the proposed R&M construction, will aid the recovery of the punctured nodes. Moreover, systematic puncturing schemes often result in optimized puncturing patterns which may have to be stored at the receiver and is not practical for mobile systems.

Hence, we show that RC SC QC LDPC codes can be derived by regular puncturing, which is similar to the approach adopted with 3GPP turbo codes, with minimal additional receiver space and computational complexity. The irregular SC QC codes constructed in the last subsection are used as the mother codes. Table III gives the puncturing pattern used in the RC SC QC LDPC codes, where 'X' denotes the punctured VNs in the protograph.

TABLE III
PUNCTURED PATTERN USED FOR RATE COMPATIBLE SCHEME.

rate = 0.45	(0,X,X,0,0,X,X,0)
rate = 0.60	(0,X,X,0,X,X,X,0)
rate = 0.72	(0,X,X,0,X,X,X,0,0,X,X,X,X,X,X,0)

The error performances of RC families of the two binary 1/3 mother SC QC LDPC codes C_1 and C_2, constructed in Examples 2 and 4, are shown in Fig. 7, where we see that codes of the C_2 family perform better than those of the C_1 family at relatively low rates. However, the C_1 family becomes superior to C_2 at higher rates. It is also observed that the family of binary RC SC QC LDPC codes performs slightly better compared to the RC family of the non-binary SC QC LDPC codes C_{nb} whose error performances are shown in Fig. 8, and also compared to their corresponding BI-AWGNC Shannon limit.

VI. Window Decoding Performance of R&M Algebraic SC QC LDPC Codes

An important advantage of the SC LDPC codes is that the band-diagonal structures of their PC matrices allow serial decoding using a sliding window [8], [25], [9]. Compared to the FSD, WD can significantly reduce the decoding latency, which is more practically implementable in applications. It has been demonstrated that with a sufficiently large window size, the WD can provide near-capacity asymptotic performance [25]. When it comes to finite-length performance, the WD of a SC LDPC code results in a significant performance gain over the corresponding LDPC block code that has the same degree distribution as the SC LDPC code (ignoring the termination effect) and block-length equal to the window size [8]. All of the above merits make WD very promising in applications when decoding SC LDPC codes.

Suppose the sliding window size (the number of VNs within the sliding window at a time) is W. With WD, the iterative message passing algorithm is operating just on the nodes and edges within the sliding window, and messages on the edges outside the sliding window are not updated. After a certain stopping rule is satisfied, the window is shifted in such a way that the first W_{sh} VNs are decoded and moved out of the sliding window. Such decoding procedure continues until all the VNs in the Tanner graph of the SC LDPC codes are decoded. The readers are referred to [9], [8] for more details regarding WD.

In the following example, we analyze the WD performance of an SC QC LDPC code over GF(2^3) constructed using the R&M method. We follow the WD strategies and the stopping rules proposed in [8]. But different from [8], we also include the BLER performance of WD in our example, since our codes are terminated SC QC LDPC codes. The maximum number of iterations $I_{max,wd}$ in the sliding window is set to 100, and the soft BER threshold [8] utilized for the stopping rule is set

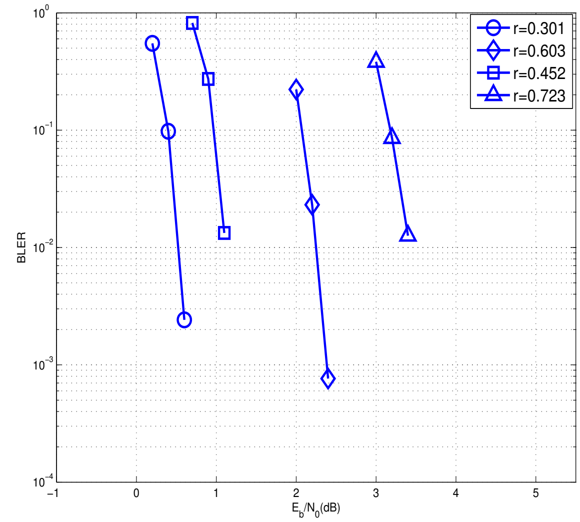

(a) BLER

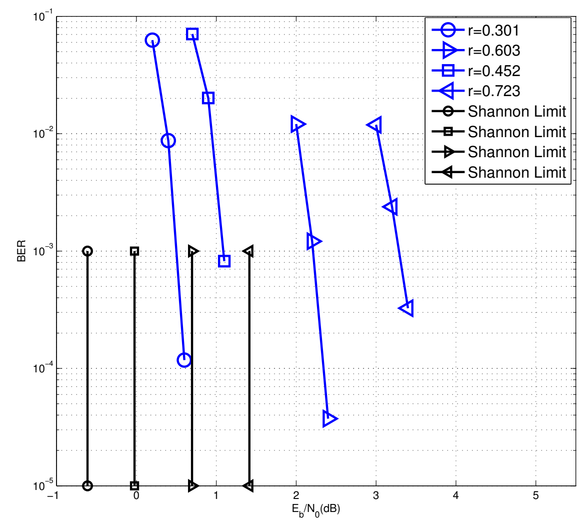

(b) BER

Fig. 8. The performance of the GF(4) RC R&M SC QC LDPC codes with information length of 6k (in bits) and regular puncturing pattern in Table III.

to 10^{-6}. Every time the iterative process within the sliding window is stopped, the window is shifted by $W_{sh} = 252$ coded symbols which are decoded. After the end of sliding window reaches the end of the codeword, we do not output all the symbols in the window as decoded symbol in one shot. Instead, we still only output the first 252 symbol in the beginning part of the window as the decoded symbol, and still 'shift' the window to the right by reducing the window length by 252. (This implementation is discussed with the first author of [8]). We continue this process until the window length is decreased to zero.

Example 5: Window Decoding of SC QC LDPC code over GF(2^3).
In this example, we construct two SC QC LDPC codes over GF(2^3) using the R&M method. One is non-periodic and de-

noted by $\mathcal{C}_{alg,rm,np}$. The other code, denoted by $\mathcal{C}_{alg,rm,p}$ has a block periodicity of $\mathcal{T}=4$.

Selection of B: For $\mathcal{C}_{alg,rm,np}$, we choose $r = 6$ and $m = n = 32$. We consider the following matrix $\mathbf{B}=\mathbf{B}_{np}$ over GF(2^6), which is constructed based on the method in [35]:

$$\mathbf{B}_{np} = \begin{bmatrix} \beta^{31} & \beta^{32} & \cdots & \beta^{62} \\ 1+\beta^{31} & 1+\beta^{32} & \cdots & 1+\beta^{62} \\ \vdots & \vdots & \ddots & \vdots \\ \beta^{30}+\beta^{31} & \beta^{30}+\beta^{32} & \cdots & \beta^{30}+\beta^{62} \end{bmatrix}, \quad (17)$$

where β is a primitive element in GF(2^6).

For $\mathcal{C}_{alg,rm,p}$, we choose $r = 6$ and $m = n = 8$. We consider the following matrix $\mathbf{B}=\mathbf{B}_p$ over GF(2^6), which is also constructed based on the method in [35]:

$$\mathbf{B}_{p} = \begin{bmatrix} \beta^{7} & \beta^{8} & \cdots & \beta^{14} \\ 1+\beta^{7} & 1+\beta^{8} & \cdots & 1+\beta^{14} \\ \vdots & \vdots & \ddots & \vdots \\ \beta^{6}+\beta^{7} & \beta^{6}+\beta^{8} & \cdots & \beta^{6}+\beta^{14} \end{bmatrix}, \quad (18)$$

where β is a primitive element in GF(2^6).

Construction of $\mathbf{W}_{base}$: For fair comparison, the same masking matrix $\mathbf{W}_{base}$ is chosen for both $\mathcal{C}_{alg,rm,np}$ and $\mathcal{C}_{alg,rm,p}$. We consider the following 41×80 protomatrix corresponding to a (3,6,40) SC protograph:

$$\mathbf{P}_{proto} = \begin{bmatrix} 1 & 2 & & & & & & & & \\ 2 & 1 & 1 & 2 & & & & & & \\ & & 2 & 1 & 1 & 2 & & & & \\ & & & & 2 & 1 & & & & \\ & & & & \ddots & \ddots & & & & \\ & & & & & & \ddots & \ddots & 1 & 2 \\ & & & & & & & & 2 & 1 \end{bmatrix}. \quad (19)$$

Since $\mathbf{P}_{proto}$ has entries greater than 1, we replace each 0,1,2 in $\mathbf{P}_{proto}$ by a 2×2 ZM, identity matrix and all-one matrix, respectively. Such replacement procedure result in the masking matrix $\mathbf{W}_{base}$ used for the R&M method. In fact, it is clear that the $\mathbf{W}_{base}$ can also be constructed using (5) with $a=b=4$, $c=2$, $L=40$ and all the 40 component regular matrices $\{\Delta_k\}$ $(0\le k<40)$ chosen to be equal to the following matrix:

$$\begin{bmatrix} 1 & 0 & 1 & 1 \\ 0 & 1 & 1 & 1 \\ 1 & 1 & 1 & 0 \\ 1 & 1 & 0 & 1 \end{bmatrix}, \quad (20)$$

R&M process and assignments of elements from GF(2^3):

Periodic codes: Using the R&M process given in Algorithm 2 on $\mathbf{B}_{np}$, we obtain a 82×160 SC array $\mathbf{H}_{sc,qc,np}$ of 63×63 CPMs and ZMs. For each CPM in $\mathbf{H}_{sc,qc}$, choose a nonzero element randomly from GF(2^3) and replace all the 1-entries in this CPM by this element. After such replacement procedure, we obtain a 82×160 SC array $\mathbf{H}_{sc,qc,nb,np}$ of 63×63 *weighted* CPMs and ZMs, which is a 5166×10080 matrix over GF(2^3). The null space of $\mathbf{H}_{sc,qc,nb}$ gives a (10080,4914) non-periodically time-varying SC QC LDPC code $\mathcal{C}_{alg,rm,np}$ over GF(2^3).

Non-periodic codes: Using the R&M process given in Algorithm 2 on $\mathbf{B}_p$, we obtain an 82×160 SC array $\mathbf{H}_{sc,qc,p}$ of 63×63 CPMs and ZMs. It follows from (6) that the block periodicity $\mathcal{T}=4$. Let $\{\Sigma_k\}_{0\le k<40}$ denote the 40 component matrices of $\mathbf{H}_{sc,qc,p}$, as defined in Sections III-B and IV-B. In order to preserve the block periodicity, the B-to-NB replacement procedure is carried out in such a way that the same B-to-NB replacement is applied on the two matrices Σ_{k_1} and Σ_{k_2} $(0\le k_1<k_2<40)$ if $k_1-k_2=4$. After such replacement procedure, we obtain a 82×160 SC array $\mathbf{H}_{sc,qc,nb,p}$ of 63×63 *weighted* CPMs and ZMs, which is a 5166×10080 matrix over GF(2^3). The null space of $\mathbf{H}_{sc,qc,nb}$ gives a (10080,4914) periodically time-varying SC QC LDPC code $\mathcal{C}_{alg,rm,p}$ over GF(2^3) with block periodicity $\mathcal{T}=4$.

It is worth mentioning that, in protograph terminologies, both of the two algebraic SC QC LDPC codes $\mathcal{C}_{alg,rm,p}$ and $\mathcal{C}_{alg,rm,np}$ can be viewed as the protograph SC LDPC codes lifted from the SC protograph corresponding to $\mathbf{P}_{proto}$ with lifting size 126.

For fair comparison, we construct another two GF(2^3) SC-LDPC codes, $\mathcal{C}_{peg,uw}$ and $\mathcal{C}_{alg,uw}$, where $\mathcal{C}_{peg,uw}$ is a (10080,4920) SC LDPC code constructed based on unwrapping a $(3,6)$-regular PEG block code over GF(2^3), and $\mathcal{C}_{alg,uw}$ is a (10080,4914) SC QC LDPC code constructed based on unwrapping a (3,6)-regular algebraic QC block code over GF(2^3), respectively. The code $\mathcal{C}_{alg,uw}$ has the same SC protograph and lifting size as $\mathcal{C}_{alg,rm,p}$ and $\mathcal{C}_{alg,rm,np}$, and has a block periodicity $\mathcal{T}=2$. The PC matrices for all of the 4 SC codes have the same size.

In the numerical Monte-Carlo simulations, two window sizes $W = 6\times 252 = 1512$ and $W = 20\times 252 = 5040$ (in terms of coded symbols) are chosen for window decoding. The results are shown in Figs. 9(a) and 9(c), respectively. Also, Fig. 9(b) shows the FSD performance with the maximum number of iterations set to 2000. Both the WD and FSD are carried out using the FFT-QSPA for reliability updating.

Firstly, we compare the two algebraic SC QC LDPC codes $\mathcal{C}_{alg,rm,np}$ and $\mathcal{C}_{alg,uw}$. We see that for both WD and FSD, in the error floor region, the R&M algebraic SC QC LDPC code $\mathcal{C}_{alg,rm,np}$ shows better performance in terms of BLER than the unwrapped algebraic SC QC LDPC code $\mathcal{C}_{alg,uw}$. If we view the FSD as a special case of WD with window size equal to the codeword length, the performance advantage of $\mathcal{C}_{alg,rm,np}$ over $\mathcal{C}_{alg,uw}$ becomes more significant at shorter window lengths. For the case of WD with $W = 1512$, the code $\mathcal{C}_{alg,rm}$ surprisingly outperforms $\mathcal{C}_{alg,uw}$ by about 0.25 dB at the BLER of 10^{-2}, which is the operating BLER for the 3GPP LTE. Therefore, we conclude that the R&M SC code $\mathcal{C}_{alg,rm,np}$ is especially desirable over the unwrapped SC code $\mathcal{C}_{alg,uw}$ for many scenarios where a short decoding latency and high decoding throughput is required.

Secondly, we compare the two algebraic SC QC LDPC codes $\mathcal{C}_{alg,rm,np}$ and $\mathcal{C}_{alg,rm,p}$. We see that for the WD, the two codes perform very close to each other. However, the periodically time-varying code $\mathcal{C}_{alg,rm,p}$ gives implementation advantages over the non-periodically time-varying code $\mathcal{C}_{alg,rm,np}$. It is also worth mentioning that, the performance gain of $\mathcal{C}_{alg,rm,np}$ and $\mathcal{C}_{alg,rm,p}$ over $\mathcal{C}_{alg,uw}$ is to a large extent attributed to the time-varying nature. Therefore, it is at the expense of increasing the window decoder implementation complexity. Hardware implementations of the WD of time-varying SC LDPC codes may need a re-configurable window decoder.

This article has been accepted for publication in a future issue of this journal, but has not been fully edited. Content may change prior to final publication. Citation information: DOI 10.1109/JSAC.2015.2504273, IEEE Journal on Selected Areas in Communications

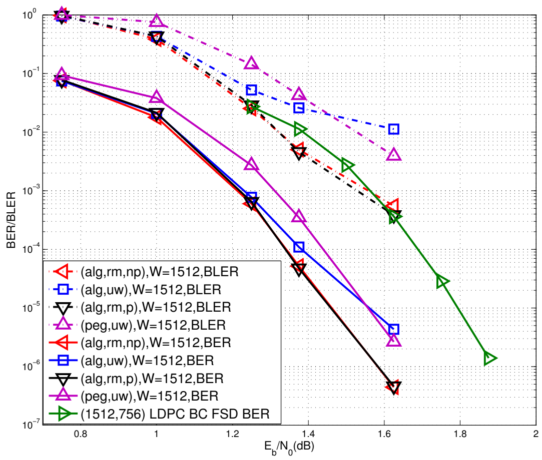

(a) WD $W = 1512$

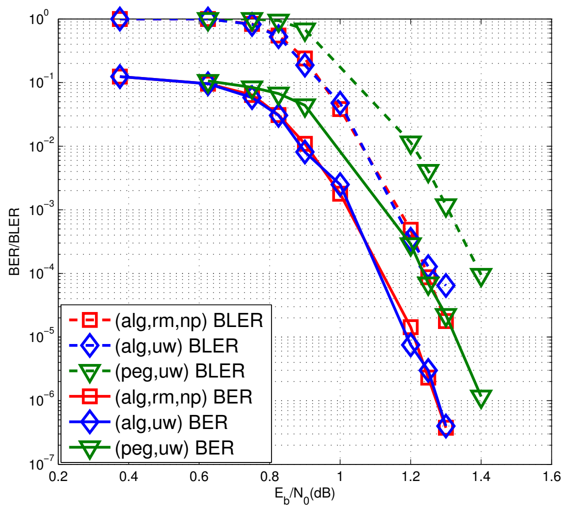

(b) FSD

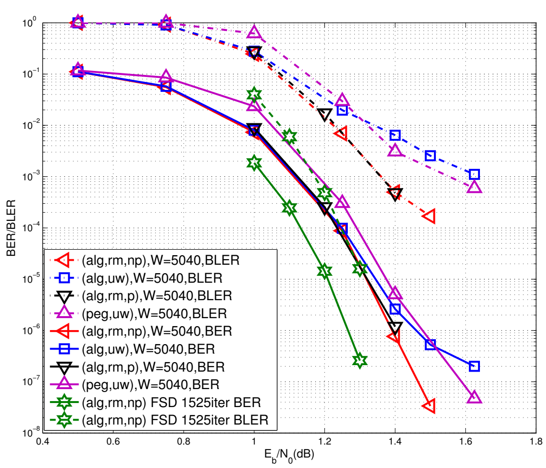

(c) WD $W = 5040$

Fig. 9. Window decoding and flooding schedule decoding performances of R&M SC codes, unwrapped SC codes, and block codes, *cf.* Example 5.

Every time after the window shifts, the window decoder is reconfigured to make it correspond to the new submatrix in the sliding window, which increases the decoder implementation complexity. The total number of the different configurations also grows proportionally to the block periodicity. However, the increase in implementation complexity of the WD of $\mathcal{C}_{alg,rm,p}$ compared to that of WD of $\mathcal{C}_{alg,uw}$ is acceptable given the notable performance gain in terms of BLER.

In addition, comparing the performances of the R&M algebraic SC QC LDPC code $\mathcal{C}_{alg,rm,np}$ and the PEG SC LDPC code $\mathcal{C}_{peg,uw}$, we see that the algebraic R&M SC QC LDPC code $\mathcal{C}_{alg,rm,np}$ outperforms $\mathcal{C}_{peg,uw}$ by about 0.15 to 0.3 dB, depending on the decoding methods. Besides, the QC structure given by the algebraic construction brings the code $\mathcal{C}_{alg,rm,np}$ significant encoding and decoding advantages that are not possessed by $\mathcal{C}_{peg,uw}$.

We also compare the WD performance with the FSD performance for $\mathcal{C}_{alg,rm,np}$, in Fig. 9(c). In order to make a fair comparison, we adjust the maximum number of iterations for FSD to make both the WD and FSD have the *same number of VN a-posteriori information updates at the worse case*. For the WD, we group all the 10080 VNs in the code $\mathcal{C}_{alg,rm}$ into 40 segments $\mathcal{V}_0, \mathcal{V}_1, ..., \mathcal{V}_{39}$. For $0 \le \lambda < 40$, each segment $\mathcal{V}_\lambda$ consisting of 252 VNs, which is the targeted (decoded) VNs for the WD at time λ. Let $\mathcal{N}_\lambda$ denote the total number of a-posteriori information updates for the VNs in segment $\mathcal{V}_\lambda$ throughout the whole WD process. Then, it is clear that $\mathcal{N}_\lambda = 252 \cdot I_{max,wd} \cdot W/W_{sh}$ for $\lambda \ge \frac{W}{W_{sh}} - 1$, and $\mathcal{N}_\lambda = 252 \cdot I_{max,wd} \cdot (\lambda + 1)$ for $\lambda < \frac{W}{W_{sh}} - 1$. For the WD with $W = 5040$, the total number of VN updates in WD in the worse case is: $\sum_{0 \le \lambda < 40} \mathcal{N}_\lambda = 252 \cdot I_{max,wd} \cdot (1 + 2 + ... + 19 + 20 * 21) = 252 \cdot I_{max,wd} \cdot 610$. For the FSD, the total number of VN updates at the worse case is $10080 \cdot I_{max,fsd}$, where $I_{max,fsd}$ is the preset maximum number of iterations for the FSD. To make these two numbers equal to each other, we need to see $I_{max,fsd} = 15.25 \cdot I_{max,wd} = 1525$. Therefore, the FSD performance included in Fig. 9(c) is assuming a maximum of 1525 FSD iterations. We see that, at the waterfall region, the WD of $\mathcal{C}_{alg,rm,np}$ does not incur much performance loss compared to the FSD. The WD with $W = 5040$ performs about 0.2 dB away from the FSD, while significantly reducing the decoding latency compared to the FSD.

Also included in Fig. 9(a) is the FSD performance of a (3,6)-regular (1512,756) algebraic QC-LDPC block code $\mathcal{C}_{bc}$ over GF(8) decoded with maximum number of iterations set to 100. In accordance with the conclusion in [8], the WD of $\mathcal{C}_{alg,rm,np}$ with $W = 1512$ significantly outperforms the FSD of $\mathcal{C}_{bc}$, while having the same decoding latency as the FSD of $\mathcal{C}_{bc}$.

VII. Conclusion and Remarks

This paper addresses the construction and analysis of finite-length binary and non-binary spatially-coupled (SC) quasi-cyclic (QC) LDPC codes. An 'replicate-and-mask' (R&M) algebraic construction of SC QC LDPC codes from an algebraic QC LDPC block code is proposed. It is shown that the R&M construction generalizes the conventional unwrapping construction of SC LDPC codes. Certain properties of the constructed R&M SC codes such as the girth, rank, and block periodicity are proved. It is verified, by numerical simulations on the AWGN channel, that the constructed algebraic R&M SC QC LDPC codes have better performance than their counterparts, such as the unwrapped algebraic SC QC LDPC codes, SC PEG LDPC codes, and block LDPC codes. R&M constructions of structured irregular SC QC LDPC codes are demonstrated and shown to have comparable performance to the 3GPP turbo codes in the waterfall region, as well as better performance at the error floor region. Also, this paper considers the design of rate-compatible families of algebraic SC QC LDPC codes suitable for incremental redundancy. It is shown that the constructed R&M SC LDPC codes are robust to regular puncturing on the AWGN channel. Performance comparisons with window decoding and flooding schedule decoding illustrated the potential decoding latency reductions and coding gains that can be achieved by adopting the proposed algebraic R&M SC QC LDPC codes.

ACKNOWLEDGEMENT

The authors would like to sincerely thank Prof. Shu Lin and Prof. Daniel Costello for their very valuable comments and discussions. They would also like to thank Mr. Kechao Huang for his very helpful discussion about window decoding implementation. The authors are very thankful to Arvind Yedla and Inyup Kang for their insightful discussions.

The first author's work is partially supported by the NSF under Grant CCF-1015548.

APPENDIX A
PROOFS OF LEMMAS AND THEOREMS

Proof of Lemma 1: We prove this lemma by contradiction. Suppose there exists a cycle of length 4 in the Tanner graph of $\mathbf{H}_{sc}$, then there must exist a 2×2 submatrix $\mathbf{P}$ of $\mathbf{H}_{sc}$, such that all the 4 elements in $\mathbf{P}$ are non-zero. It is clear that for any non-zero element $h_{sc,i,j}$ $(0 \leq i < S, 0 \leq j < T)$ in $\mathbf{H}_{sc}$, we have $h_{sc,i,j} = h_{rep,i,j}$ and $w_{i,j} = 1$. Suppose $\mathbf{P}$ is obtained by taking the intersections of the rows i_1, i_2 and the columns j_1, j_2 in $\mathbf{H}_{sc}$, then we have

$$\mathbf{P} = \begin{bmatrix} h_{rep,i_1,j_1} & h_{rep,i_1,j_2} \\ h_{rep,i_2,j_1} & h_{rep,i_2,j_2} \end{bmatrix}, \text{ i.e.,}$$

$$\mathbf{P} = \begin{bmatrix} h_{i_1 \bmod M, j_1 \bmod N} & h_{i_1 \bmod M, j_2 \bmod N} \\ h_{i_2 \bmod M, j_1 \bmod N} & h_{i_2 \bmod M, j_2 \bmod N} \end{bmatrix}.$$

Also, we have $w_{i_1,j_1} = w_{i_1,j_2} = w_{i_2,j_1} = w_{i_2,j_2} = 1$. Then, the condition given in the lemma ensures that $\mathbf{P}$ can also be viewed as a 2×2 submatrix of $\mathbf{H}$. However, since $\mathbf{H}$ has a Tanner graph with girth at least 6, any 2×2 submatrix of $\mathbf{H}$ must has at least one zero element, which contradicts the assumption that all the 4 elements of $\mathbf{P}$ are non-zero. Thus, the lemma follows. ∎

Proof of Lemma 2: We prove this lemma by contradiction. For simplicity, in this proof we do not distinguish between the Tanner graphs and their corresponding PC matrices. Suppose there is a cycle of length $2t$ in $\mathbf{H}_{sc}$, denoted by $C(2t)$, as follows: $x_1 \to y_1 \to x_2 \to y_2 \to \cdots \to x_t \to y_t \to x_1$, where $x_1, x_2, ..., x_t$ denote the row (CN) labels for $\mathbf{H}_{sc}$ and $y_1, y_2, ..., y_t$ denote the column (VN) labels for $\mathbf{H}_{sc}$. For $0 \leq i < t$, let $x'_i = x_i \bmod M$ and $y'_i = y_i \bmod N$. Based on the relationship among $\mathbf{H}_{sc}$, $\mathbf{H}_{rep}$ and $\mathbf{H}$, it is clear that the sequence $x'_1 \to y'_1 \to x'_2 \to y'_2 \to \cdots \to x'_t \to y'_t \to x'_1$ is a closed loop in $\mathbf{H}$, denoted by $C'(2t)$, where $x'_1, x'_2, ..., x'_t$ denote the row labels for $\mathbf{H}$ and $y'_1, y'_2, ..., y'_t$ denote the column labels for $\mathbf{H}$. Moreover, the conditions given in the lemma ensure that all the CNs $x'_1, x'_2, ..., x'_t$ in $\mathbf{H}$ are distinct, and all the VNs $y'_1, y'_2, ..., y'_t$ in $\mathbf{H}$ are distinct. Hence, $C'(2t)$ is a cycle with length $2t$ in $\mathbf{H}$. This proves the lemma. ∎

Proof of Lemma 3: We have $\psi_{i,j,k} = \sigma'_{i,j} \cdot h_{rep,i+kC,j+kB}$ for $0 \leq i < A$, $0 \leq j < B$ and $0 \leq k < L$. If $k_2 - k_1 = \mathcal{T} = \frac{MN}{GCD(BM,CN)}$, we have $\psi_{i,j,k_2} = \sigma'_{i,j} \cdot h_{rep,i+k_2C,j+k_2B} = \sigma'_{i,j} \cdot h_{rep,i+k_1C+\mathcal{T}C,j+k_1B+\mathcal{T}B}$, where $\mathcal{T}C = \frac{MNC}{GCD(BM,CN)} = M \cdot \frac{NC}{GCD(BM,CN)}$ is a multiple of M, and $\mathcal{T}B = \frac{MNB}{GCD(BM,CN)} = N \cdot \frac{MB}{GCD(BM,CN)}$ is a multiple of N. Since $\mathbf{H}_{rep}$ is a semi-infinite array of $\mathbf{H}$ of size $M \times N$, we have $h_{rep,i+k_1C+\mathcal{T}C,j+k_1B+\mathcal{T}B} = h_{rep,i+k_1C,j+k_1B}$ for $0 \leq i < A$ and $0 \leq j < B$. Then, we have $\psi_{i,j,k_2} = \sigma'_{i,j} \cdot h_{rep,i+k_1C,j+k_1B} = \psi_{i,j,k_1}$ for $0 \leq i < A$ and $0 \leq j < B$. Therefore, we have $\Psi_{k_1} = \Psi_{k_2}$.

On the other hand, we can verify that $\mathcal{T} = \frac{MN}{GCD(BM,CN)}$ is the smallest choice of $\mathcal{T}$ that can ensure that $\Psi_k = \Psi_{k+\mathcal{T}}$ for any k, given M, N, A, B and C. In order to show that, we note that $\psi_{i,j,k+\mathcal{T}} = \sigma'_{i,j} \cdot h_{rep,i+kC+\mathcal{T}C,j+kB+\mathcal{T}B}$ for $0 \leq i < A$, $0 \leq j < B$ and $0 \leq k < L$. Therefore, we need to choose $\mathcal{T}$ such that $\mathcal{T}C$ is a multiple of M and $\mathcal{T}B$ is a multiple of N, to ensure $\psi_{i,j,k+\mathcal{T}} = \psi_{i,j,k}$. Suppose $\mathcal{T}C = \kappa_1 M$ and $\mathcal{T}B = \kappa_2 N$, then we have $\frac{\kappa_1}{\kappa_2} = \frac{CN}{BM}$. Since C, B, M, N are given, we need to find the smallest possible choices of positive integers κ_1 and κ_2 with $\frac{\kappa_1}{\kappa_2} = \frac{CN}{BM}$. Therefore, we need to choose $\kappa_1 = \frac{CN}{GCD(CN,BM)}$ and $\kappa_2 = \frac{BM}{GCD(CN,BM)}$, and the corresponding smallest possible choice of $\mathcal{T} = \frac{\kappa_1 M}{C} = \frac{MN}{GCD(CN,BM)}$. ∎

Proof of Theorem 1: To apply Theorem 1, we need to prove that $M = m(q-1)$ does not divide $i_1 - i_2$ and $N = n(q-1)$ does not divide $j_1 - j_2$, for any i_1, i_2, j_1, j_2 with $0 \leq i_1 < i_2 < S = s(q-1)$, $0 \leq j_1 < j_2 < T = t(q-1)$, and $w_{qc,i_1,j_1} = w_{qc,i_1,j_2} = w_{qc,i_2,j_1} = w_{qc,i_2,j_2} = 1$. Let $i'_1 = \lfloor i_1/(q-1) \rfloor$, $i'_2 = \lfloor i_2/(q-1) \rfloor$, $j'_1 = \lfloor j_1/(q-1) \rfloor$, and $j'_2 = \lfloor j_2/(q-1) \rfloor$. Then, it follows from the relationship between $\mathbf{W}_{qc}$ and $\mathbf{W}_{base}$ that $w_{base,i'_1,j'_1} = w_{base,i'_1,j'_2} = w_{base,i'_2,j'_1} = w_{base,i'_2,j'_2} = 1$. Suppose M divides $i_1 - i_2$, then $(i_1 \bmod (q-1)) = (i_2 \bmod (q-1))$. Since $i_1 - i_2 = (q-1)(i'_1 - i'_2) + (i_1 \bmod (q-1)) - (i_2 \bmod (q-1))$, we have $i'_1 - i'_2 = (i_1 - i_2)/(q-1)$, which is divisible by m and contradicts the condition given in the theorem. Similarly, we can prove that $N = n(q-1)$ does not divide $j_1 - j_2$. ∎

Proof of Theorem 2: Let P be an arbitrary 2×2 all-one submatrix of $\mathbf{W}_{base}(a, b, c, L)$, and suppose P is obtained by taking the intersection of rows i_1, i_2 and columns j_1, j_2 of $\mathbf{W}_{base}(a, b, c, L)$. We can verify by inspection that $|i_2 - i_1| \leq m$ and $|j_2 - j_1| \leq n$ must hold if $a \leq m$ and $\lceil (a-1)/c \rceil b \leq n$, which implies that the condition of Theorem 1 is satisfied. This proves the theorem. ∎

Proof of Theorem 3: The largest possible constraint length of the constructed $\mathbf{H}_{sc,qc}$ is $(q-1)b\lceil a/c \rceil \leq n(q-1) = N$, which ensures that the condition (2) in Lemma 2 is satisfied. Similarly, $a \leq m$ ensures that the condition (1) in Lemma 2 is satisfied. Thus we complete the proof. ∎

Proof of Theorem 4: Since $\mathbf{B}$ does not have any zero entries, $\mathbf{B}_{sc}^{\circ 0}$ is a binary matrix that can be obtained by simply replacing each non-zero element in $\mathbf{B}_{sc}$ by 1, i.e., $\mathbf{B}_{sc}^{\circ 0} = \mathbf{W}_{base}(a, b, c, L)$. Suppose we apply the following elementary row operations to $\mathbf{B}_{sc}^{\circ 0}$: we add the 0-th row to the next $(a-1)$ rows, say rows $1, 2, ..(a-1)$, then add the c-th row to the next $(a-1)$ rows, say rows $c+1, c+2, ..., c+(a-1)$, then add the $2c$-th row to the next $(a-1)$ rows, say rows $2c+1, 2c+2, ..., 2c+(a-1)$. We continue this process until we add the $(c(L-1))$-th rows to the next $(a-1)$ rows, say rows $(L-1)c+1, (L-1)c+2, ..., (L-1)c+(a-1)$, which are also the last $a-1$ rows in $\mathbf{B}_{sc}^{\circ 0}$. After such row operations, only L rows in $\mathbf{B}_{sc}^{\circ 0}$, say rows $0, c, ..., (L-1)c$, remain to be non-zero and clearly these L rows are linearly independent. Hence, we have $\mathrm{rank}(\mathbf{B}_{sc}^{\circ 0}) = L$. Then the theorem follows from (7). ■

REFERENCES

[1] K. Liu, M. El-Khamy, J. Lee, I. Kang, and A. Yedla, “Non-binary algebraic spatially-coupled quasi-cyclic LDPC codes,” in *Proc. IEEE International Symposium on Information Theory (ISIT)*, Jun. 2014, pp. 511–515.

[2] A. J. Felstrom and K. Zigangirov, “Time-varying periodic convolutional codes with low-density parity-check matrix,” *IEEE Trans. Inf. Theory*, vol. 45, no. 6, pp. 2181–2191, 1999.

[3] S. Kudekar, T. Richardson, and R. Urbanke, “Threshold saturation via spatial coupling: Why convolutional LDPC ensembles perform so well over the BEC,” *IEEE Trans. Inf. Theory*, vol. 57, no. 2, pp. 803–834, 2011.

[4] S. Kudekar, C. Measson, T. Richardson, and R. Urbankez, “Threshold saturation on BMS channels via spatial coupling,” in *Proc. 6th International Symposium on Turbo Codes and Iterative Information Processing (ISTC)*, 2010, pp. 309–313.

[5] A. Yedla, Y.-Y. Jian, P. Nguyen, and H. Pfister, “A simple proof of threshold saturation for coupled scalar recursions,” in *Proc. 7th International Symposium on Turbo Codes and Iterative Information Processing (ISTC)*, 2012, pp. 51–55.

[6] M. Lentmaier, A. Sridharan, D. J. Costello Jr, and K. Zigangirov, “Iterative decoding threshold analysis for LDPC convolutional codes,” *IEEE Trans. Inf. Theory*, vol. 56, no. 10, pp. 5274–5289, 2010.

[7] R. G. Gallager, “Low-density parity-check codes,” *IRE Trans. Inf. Theory*, vol. 8, no. 1, pp. 21–28, 1962.

[8] K. Huang, D. G. M. Mitchell, L. Wei, X. Ma, and D. Costello, “Performance comparison of LDPC block and spatially coupled codes over GF (q),” *IEEE Trans. Commun.*, vol. 63, no. 3, pp. 592–604, March 2015.

[9] A. Iyengar, M. Papaleo, P. Siegel, J. Wolf, A. Vanelli-Coralli, and G. Corazza, “Windowed decoding of protograph-based LDPC convolutional codes over erasure channels,” *IEEE Trans. Inf. Theory*, vol. 58, no. 4, pp. 2303–2320, Apr. 2012.

[10] M. Fossorier, “Quasi cyclic low-density parity-check codes from circulant permutation matrices,” *IEEE Trans. Inf. Theory*, vol. 50, no. 8, pp. 1788–1793, 2004.

[11] Z. Li, L. Chen, L. Zeng, S. Lin, and W. Fong, “Efficient encoding of quasi-cyclic low-density parity-check codes,” *IEEE Trans. Commun.*, vol. 53, no. 11, pp. 1973–1973, 2005.

[12] Y. Chen and K. Parhi, “Overlapped message passing for quasi-cyclic low-density parity check codes,” *IEEE Trans. Circuits Syst. I*, vol. 51, no. 6, pp. 1106–1113, 2004.

[13] W. Ryan and S. Lin, *Channel Codes: Classical and Modern*. Cambridge University Press, 2009.

[14] L. Lan, L. Zeng, Y. Tai, L. Chen, S. Lin, and K. Abdel-Ghaffar, “Construction of quasi-cyclic LDPC codes for AWGN and binary erasure channels: A finite field approach,” *IEEE Trans. Inf. Theory*, vol. 53, no. 7, pp. 2429–2458, Jul. 2007.

[15] L. Zhang, Q. Huang, S. Lin, K. Abdel-Ghaffar, and I. F. Blake, “Quasi-cyclic LDPC codes: an algebraic construction, rank analysis, and codes on Latin squares,” *IEEE Trans. Commun.*, vol. 58, no. 11, pp. 3126–3139, 2010.

[16] L. Dolecek, D. Divsalar, Y. Sun, and B. Amiri, “Non-binary protograph-based LDPC codes: Enumerators, analysis, and designs,” *Information Theory, IEEE Transactions on*, vol. 60, no. 7, pp. 3913–3941, 2014.

[17] D. Mitchell, R. Smarandache, M. Lentmaier, and D. Costello, “Quasi-cyclic asymptotically regular LDPC codes,” in *Proc. IEEE Information Theory Workshop (ITW)*, 2010, pp. 1–5.

[18] X.-Y. Hu, E. Eleftheriou, and D.-M. Arnold, “Regular and irregular progressive edge-growth Tanner graphs,” *IEEE Trans. Inf. Theory*, vol. 51, no. 1, pp. 386–398, 2005.

[19] V. A. Chandrasetty, S. J. Johnson, and G. Lechner, “Memory efficient decoders using spatially coupled quasi-cyclic LDPC codes,” *CoRR*, vol. abs/1305.5625, 2013.

[20] M. Hagiwara, K. Kasai, H. Imai, and K. Sakaniwa, “Spatially coupled quasi-cyclic quantum LDPC codes,” in *Proc. IEEE International Symposium on Information Theory (ISIT)*, 2011, pp. 638–642.

[21] A. Pusane, R. Smarandache, P. Vontobel, and D. Costello, “Deriving good LDPC convolutional codes from LDPC block codes,” *IEEE Trans. Inf. Theory*, vol. 57, no. 2, pp. 835–857, 2011.

[22] M. Lentmaier, D. Truhachev, and K. S. Zigangirov, “To the theory of low-density convolutional codes. ii,” *Problems of Information Transmission*, vol. 37, no. 4, pp. 288–306, 2001.

[23] Q. Diao, Q. Huang, S. Lin, and K. Abdel-Ghaffar, “A matrix-theoretic approach for analyzing quasi-cyclic low-density parity-check codes,” *IEEE Trans. Inf. Theory*, vol. 58, no. 6, pp. 4030–4048, 2012.

[24] F. Kschischang and B. Frey, “Iterative decoding of compound codes by probability propagation in graphical models,” *IEEE J. Sel. Areas Commun.*, vol. 16, no. 2, pp. 219–230, Feb. 1998.

[25] L. Wei, T. Koike-Akino, D. Mitchell, T. Fuja, and D. J. Costello Jr, “Threshold analysis of non-binary spatially-coupled LDPC codes with windowed decoding,” in *Information Theory (ISIT), 2014 IEEE International Symposium on*, June 2014, pp. 881–885.

[26] A. Piemontese, A. G. Amat, and G. Colavolpe, “Nonbinary spatially-coupled LDPC codes on the binary erasure channel,” in *Proc. IEEE International Conference on Communications (ICC)*, 2013, pp. 3270–3274.

[27] J. Thorpe, “Low-density parity-check (LDPC) codes constructed from protographs,” *IPN progress report*, vol. 42, no. 154, pp. 42–154, 2003.

[28] R. A. Horn and C. R. Johnson, *Matrix Analysis*. Cambridge University Press, 2012.

[29] Y. Kou, S. Lin, and M. Fossorier, “Low-density parity-check codes based on finite geometries: a rediscovery and new results,” *IEEE Trans. Inf. Theory*, vol. 47, no. 7, pp. 2711–2736, Nov. 2001.

[30] Y. Y. Tai, L. Lan, L. Zeng, S. Lin, and K. A. S. Abdel-Ghaffar, “Algebraic construction of quasi-cyclic LDPC codes for the AWGN and erasure channels,” *IEEE Trans. Commun.*, vol. 54, no. 10, pp. 1765–1774, Oct. 2006.

[31] S. Lin, J. Xu, I. Djurdjevic, and H. Tang, “Hybrid construction of

This article has been accepted for publication in a future issue of this journal, but has not been fully edited. Content may change prior to final publication. Citation information: DOI 10.1109/JSAC.2015.2504273, IEEE Journal on Selected Areas in Communications

LDPC codes," in *Proc. 40th Allerton Conf. Communication, Control, and Computers*, 2002, pp. 1149–1158.

[32] J. Li, K. Liu, S. Lin, K. Abdel-Ghaffar, and W. E. Ryan, "An unnoticed strong connection between algebraic-based and protograph-based LDPC codes," in *2015 Information Theory and Applications Workshop (ITA)*.

[33] Q. Huang, K. Liu, and Z. Wang, "Low-density arrays of circulant matrices: Rank and row-redundancy analysis, and quasi-cyclic LDPC codes," *CoRR*, vol. abs/1202.0702, 2012.

[34] J. Li, K. Liu, S. Lin, and K. Abdel-Ghaffar, "A matrix-theoretic approach to the construction of non-binary quasi-cyclic LDPC codes," *IEEE Trans. Commun.*, vol. 63, no. 4, pp. 1057–1068, April 2015.

[35] ——, "Algebraic quasi-cyclic LDPC codes: Construction, low error-floor, large girth and a reduced-complexity decoding scheme," *IEEE Trans. Commun.*, vol. 62, no. 8, pp. 2626–2637, Aug. 2014.

[36] M. El-Khamy, J. Hou, and N. Bhushan, "Design of rate-compatible structured LDPC codes for hybrid ARQ applications," *IEEE J. Sel. Areas Commun.*, vol. 27, no. 6, pp. 965–973, 2009.

[37] D. Divsalar, S. Dolinar, J. Thorpe, and C. Jones, "Constructing LDPC codes from simple loop-free encoding modules," in *Proc. IEEE International Conference on Communications (ICC)*, vol. 1, 2005, pp. 658–662.

[38] D. Mitchell, R. Smarandache, and J. Costello, D.J., "Quasi-cyclic LDPC codes based on pre-lifted protographs," *Information Theory, IEEE Transactions on*, vol. 60, no. 10, pp. 5856–5874, Oct 2014.

[39] H. Uchikawa, K. Kasai, and K. Sakaniwa, "Design and performance of rate-compatible non-binary LDPC convolutional codes," *IEICE TRANSACTIONS on Fundamentals of Electronics, Communications and Computer Sciences*, vol. 94, no. 11, pp. 2135–2143, 2011.

[40] H. Zhou, D. Mitchell, N. Goertz, and D. Costello, "Robust rate-compatible punctured LDPC convolutional codes," *IEEE Trans. Commun.*, vol. 61, no. 11, pp. 4428–4439, Nov. 2013.

[41] S. Kudekar, T. Richardson, and R. Urbanke, "Spatially coupled ensembles universally achieve capacity under belief propagation," in *Proc. 2012 IEEE International Symposium on Information Theory (ISIT)*, pp. 453–457.

Keke Liu received the B.E. and M.E. degrees from Beijing Institute of Technology, Beijing, China, in 2007 and 2009, respectively, both in electrical engineering. From 2009 to 2010, he joined Datang Mobile, Beijing, China, as a Physical Protocol Engineer. He received his Ph.D degree in electrical and computer engineering from the University of California, Davis, CA, USA, in 2015. He is currently a Research Engineer in Avago Technologies, San Jose, CA. His research interests are in the general area of error control coding and signal processing for communication and storage systems.

Mostafa El-Khamy received Ph.D. and M.S. degrees in Electrical Engineering from the California Institute of Technology (Caltech), USA in 2006 and 2003, respectively. He received M.Sc. and B.Sc. degrees from Alexandria University, Egypt in 2001 and 1999, respectively. From 2006 to 2008, he was at Qualcomm R&D, San Diego, where he designed new femtocell technologies for 3GPP systems. In 2008, he joined the faculty of the Electrical Engineering Department at Alexandria University, Egypt, where he has been appointed Associate Professor. He has also held adjunct faculty positions at Virginia Tech. MENA, University of Ottawa, German University in Cairo, and Egypt-Japan University for Science and Technology. Since 2011, he has been with Samsung Modem R&D, USA, where he is currently a Principal Engineer and works on the design and research of algorithms for wireless modems and application processors.

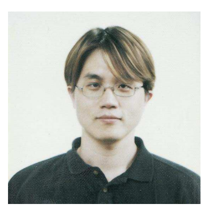

Jungwon Lee is a Senior Director at Samsung Modem R&D in San Diego, CA, in charge of a systems group for cellular and connectivity chips. He is also currently an Associate Adjunct Professor at UCSD in San Diego, CA. He received his PhD degree in Electrical Engineering from Stanford University in 2005. From 2003 to 2010, he was with Marvell Semiconductor Inc., as a Principal Engineer, where he developed HD Radio, Bluetooth, WiFi, WiMAX, and LTE chips. Since 2010, he has been with Samsung USA. Dr. Lee has co-authored more than 80 papers and holds over 200 US patents. He is a Senior Member of the IEEE.